RAPID TRAVERSAL OF 3 / 3 RADIAL RESONANCE NEAR THE CENTER OF A SECTOR FOCUSED CYCLOTRON

Thesis for the Degree of M. S.
MICHIGAN STATE UNIVERSITY

Joe Earl Stover

1960

RAPID TRAVERSAL OF 3/3 RADIAL RESONANCE NEAR THE CENTER OF A SECTOR FOCUSED CYCLOTRON

By

JOE EARL STOVER

AN ABSTRACT

Submitted to the College of Science and Arts of
Michigan State University of Agriculture and
Applied Science in partial fulfillment of
the requirements for the degree of

MASTER OF SCIENCE

Department of Physics

1960

Approved H. G. Blosser
Assoc. Prof. of Physics

JOE EARL STOVER

ABSTRACT

A nonisochronous average magnetic field for a three sector cyclotron is determined numerically that will give adequate axial focusing to a proton accelerated by an energy gain per revolution of 280 kev, without excessive phase slip.

The effects, on a beam of accelerated protons, of the traversal of the 3/3 radial resonance which are introduced by using this average magnetic field are investigated by use of the Michigan State University's digital computer, the MISTIC. It is found that a beam of 70-kev protons a half inch wide can be accelerated through this radial resonance without severe beam distortion.

RAPID TRAVERSAL OF 3/3 RADIAL RESONANCE NEAR THE CENTER OF A SECTOR FOCUSED CYCLOTRON

By

JOE EARL STOVER

A THESIS

Submitted to the College of Science and Arts of
Michigan State University of Agriculture and
Applied Science in partial fulfillment of
the requirements for the degree of

MASTER OF SCIENCE

Department of Physics

1960

ACKNOWLEDGMENTS

I wish to express my sincere appreciation to Dr. H. B. Blosser and Dr. M. M. Gordon for their advice and suggestions during the progress of this work.

I am grateful to Dr. H. G. Blosser and T. R. Arnette for furnishing the necessary computer programs and to the United States Atomic Energy Commission for making this work financially possible.

TABLE OF CONTENTS

Introduction 1

Units and Coordinates 4

Axial Focusing and Nonisochronism 5

Radial Stability and Resonance Traversal 27

Beam Distortion 42

Conclusion 59

Appendix 60

Bibliography 63

LIST OF FIGURES

Figure		Page
1.	The magnetic field in the medial plane	17
2.	The axial focusing of a three sector magnetic field	18
3.	The flutter of the magnetic field	19
4.	The axial focusing frequency of the isochronous magnetic field	20
5.	The average magnetic field necessary for a constant ν_z.	21
6.	The nonisochronous average magnetic field with acceptable phase slip	22
7.	The axial focusing frequency of a proton in the nonisochronous field	23
8.	The phase slip for a proton with an energy gain per revolution of 280 kev.	24
9.	The axial motion of a proton in the nonisochronous field.	25
10.	The amplitude damping of the axial motion	26
11.	The radial oscillation frequency of a proton in the nonisochronous magnetic field	37
12.	The stable and unstable trajectories in the median plane	38
13.	A phase diagram near resonance for a three sector magnetic field	39
14.	The stable regions at energies near resonance	40
15.	A phase plot 220 kev below resonance	41
16.	The distortion of a 0.27 inch central beam	50
17.	The initial conditions for protons accelerated and decelerated from resonance	51
18.	The distortion three revolutions above resonance	52

Figure Page

19. The distortion five revolutions above resonance 53

20. The distortion seven revolutions above resonance 54

21. The distortion nine revolutions above resonance 55

22. The distortion two revolutions below resonance 56

23. The distortion four revolutions below resonance 57

24. The distortion five revolutions below resonance 58

INTRODUCTION

The performance and energy of conventional, fixed frequency cyclotrons (i. e. those with azimuthally uniform magnetic fields) are severely curtailed by the contradictory requirements placed on the magnetic field shape by the separate considerations of focusing and acceleration. These requirements are: (1) The magnetic field should increase as a function of radius in order to maintain constant orbital frequency for particles. (2) The magnetic field should decrease as a function of radius in order to give axial focusing.

In 1938 L. H. Thomas (1) proposed a cyclotron (now commonly called a sector focused cyclotron) which employs azimuthal variation in the magnetic field in such a way as to satisfy both focusing and acceleration requirements. The introduction of sectors into the field introduces additional terms into the Kerst-Serber equations (2) for the focusing oscillation frequencies. These terms, which give axial focusing, depend upon the mean square variation of the field about a circle from its mean. Constant orbital frequency for particles (called isochronism) is maintained by increasing the average magnetic field as a function of radius in order to compensate for an accelerated particle's relativistic mass increase.

Due to restrictions imposed on the possible shapes of magnetic fields by Maxwell's equations, the isochronous average field gives rise to axial defocusing forces. Sector focusing will overcompensate

for this situation at large radii. However, the mean square variation of the field from its mean must tend to zero as the radius approaches zero, hence axial defocusing is to be expected at small radii. Axial focusing in this region has been successfully enhanced in the Delft (3) and Illinois (4) four sector cyclotrons by the abandonment of isochronism at small radii.

Cohen (5) suggested that the following procedures be used to investigate the feasibility of overcoming axial defocusing at small radii: (1) the numerical construction of an average magnetic field to supplement the axial focusing in the central region, (2) an investigation of the feasibility of the traversal of the radial oscillation resonance which is necessitated by features of this average field. In this thesis, these suggested procedures are carried out for the three sector magnetic field shown in figure 1.

The numerical calculations to determine the appropriate average magnetic field are based on formulas obtained from the smooth approximation (6). These simple formulas are often rather inaccurate, but they are useful for estimates. The orbital properties of ions in the magnetic field obtained are determined from a sequence of computer runs of the Michigan State University digital computer, the MISTIC.

The two principal computer programs which are used are the "equilibrium orbit code" (7) and the "general orbit code" (8). These programs accurately determine the desired orbital properties by integration of the particles' equations of motion. The equilibrium

orbit code takes a given median plane field and calculates the desired properties of the equilibrium orbits and the small amplitude oscillation frequencies as a function of energy. The general orbit code is used to track ions initially displaced from their equilibrium orbits. This code is also used to simulate acceleration by increasing the ions' energy at specified azimuthal angles, so that the effects of resonance traversal can be investigated.

UNITS AND COORDINATES

For convenience, cyclotron units as defined by Gordon and Welton (9) are used throughout this thesis. These are dimensionless, relativistic units well suited to cyclotron work. The rest mass, M_o, and the velocity of light, c, are taken as unit mass and velocity. Since the cyclotron considered here is a fixed-frequency accelerator, the unit time is defined in terms of this frequency as $\tau = \frac{2\pi}{\omega}$. For a particle with charge e, the magnetic field unit is

$$B = \frac{M_o c \omega_o}{e}$$

and the unit length is $a = c/\omega$.

For a proton in the magnetic field considered in this thesis

$$a = 90.4 \text{ inches} = 229.4 \text{ cm}$$

$$1/\tau = 12.18 \times 10^{-10} \text{ sec}^{-1}$$

The axial and radial oscillation frequencies ν_z and ν_r are given as the ratios of the actual frequencies of oscillation to the fixed frequency of the cyclotron.

A right cylindrical coordinates system is used with the origin located at the geometric center of the magnetic field. The z = 0 plane is taken as the plane of symmetry of the field, parallel to the pole face of the magnet.

SECTION I

AXIAL FOCUSING AND NONISOCHRONISM

Consider a magnetic field which has the property that there is a plane such that the field at all points in the plane is perpendicular to the plane. This plane of symmetry is called the median plane and is taken to be the z = 0 plane in cylindrical coordinates. There exists (10) a closed curve, called the equilibrium orbit, in this plane along which a particle with a certain momentum can move. In order to be usable as a guide field for accelerators, the magnetic field must be such that the motion of a particle near the equilibrium orbit is stable in the following sense: if a particle, whose momentum is appropriate to the given equilibrium orbit, is started with a small initial displacement and small initial angle from the equilibrium orbit, it will remain near the equilibrium orbit for all time.

Consider a charged particle moving between magnetic poles which produce a field in the z = 0 plane shown in figure 1. If the particle moves in this plane of symmetry it will experience no force in the z direction. However, for a charged particle with a small z displacement from its equilibrium orbit a z component of the magnetic force is present. Unless this is a restoring force which will cause the particle to oscillate about the median plane, its axial motion is unstable.

The axial force on the particle is given in cylindrical coordinates by

$$F_z = eV_r B_\theta - eV_\theta Br \qquad [1]$$

where e is the particle's charge, V_r and V_θ are the radial and azimuthal components of its velocity, respectively; and B_θ and B_r are the azimuthal and radial components of the magnetic field at the location of the particle.

Consider the second term on the right side of equation [1]. If the expression for the magnetic field is expanded in a Taylor's series about the median plane, equation [2] is obtained.

$$B_r(r, \theta, z) = B_r(r, \theta, 0) + z\frac{\partial B_r(r, \theta, z)}{\partial z}\bigg|_{z=0} + \ldots . \qquad [2]$$

Due to symmetry of the field about the z = 0 plane the first term in equation [2] is zero. Maxwell's equations give curl B = 0 in this region or,

$$\frac{\partial B_r}{\partial z} = \frac{\partial B_z}{\partial r} \qquad [3]$$

Hence the second term in equation [1] is, to the first order, given by

$$-eV_\theta z\frac{\partial B_z}{\partial r}\bigg|_{z=0} \qquad [4]$$

It is the axial force averaged around the particle's orbit that determines the stability of the motion. If the average field given by

$$\langle B_z \rangle = \frac{1}{2\pi}\int_0^{2\pi} B_z(r, \theta)d\theta \qquad [5]$$

is isochronous, its partial derivative with respect to r is positive, then axial defocusing is obtained from this term.

The first term in equation [1] is the axial focusing force proposed by Thomas (1). The basic concepts of this sector focusing can be understood by consideration of a simple example. Consider the cyclotron magnet to be composed of three wedge shaped magnets, each with uniform magnetic field over the region of the wedge and a much weaker uniform field interposed between the wedges, as shown in figure 2. It can be seen from the geometry that as a charged particle enters the strong field region the radial component of its velocity is positive. The curvature of the magnetic lines at the edge of the magnetic wedge is shown in figure 2. A particle with a trajectory not in the median plane will encounter an azimuthal component of the magnetic field whose direction depends on the side of the median plane in which the particle is moving. For either positive or negative z, the cross product of the radial component of the velocity and the azimuthal component of the magnetic field is in a direction such as to give a restoring axial force. In the region where the particle leaves the magnet, both the radial component of the velocity and the azimuthal component of the magnetic field have changed directions, thereby giving axial focusing.

In principle, it appears that the focusing forces derived from the azimuthal variations in the magnetic field could be made of sufficient strength to overcompensate for the defocusing forces arising from the radial variation in the isochronous magnetic field. However, in actual practice this cannot be done at small radii. Detailed analysis (6)

shows that this focusing strength is specified by the mean square deviation of the field about a circle from its mean. This deviation which is called the flutter can be made as large as necessary at large radii by proper azimuthal variation in the magnetic field but for continuous fields must equal zero at r = 0; hence it is small for small radii.

With the above principles in mind, the axial motion of an ion in a sector focused cyclotron can be discussed. Figure 1 shows a "contour map" of the magnetic field to be considered. This plot was obtained from measured magnetic field values of a scale model of the magnet for the proposed Michigan State University cyclotron described elsewhere (17). It is a three sector, weak spiraled magnet designed for a strictly isochronous average magnetic field which is given by

$$\langle B(r) \rangle = \frac{M_o \omega}{e\left[1 - \frac{r^2\omega^2}{c^2}\right]^{1/2}} \qquad [5A]$$

where M_o and e are the rest mass and the charge, respectively, c is the velocity of light and ω is the orbital frequency. The flutter, F, as defined above is shown as a function of radius in figure 3. The axial focusing frequency, ν_z, for a proton in the isochronous magnetic field is shown in figure 4. The axial focusing frequency was obtained from orbit integration by digital computer and is quite accurate.

It is noted from figure 3 that F is zero at r = 0 and quite small at small radii. It then increases rapidly with radius. It is seen from figure 4 that ν_z has a relatively constant value over a large range of r values, but falls off rapidly near the center of the field. There is defocusing at small radii.

This behavior of the axial focusing frequency can be understood in light of the approximate equation of motion for an ion with a small axial displacement from its equilibrium orbit which is given by several authors as (6, 12)

$$\frac{d^2z}{d\theta^2} + \nu_z^2 z = 0 \qquad [6]$$

where ν_z^2 is given by the smooth approximation as

$$\nu_z^2 = -\frac{r}{<B>}\frac{d<B>}{dr} + F(1 + 2\tan^2\alpha) \qquad [7]$$

where $<B>$ is the average field, F is the flutter and α is the sector spiral angle. The spiral is weak in the field considered here, hence the last term in equation [7] can be neglected for approximate calculations and equation [7] becomes

$$\nu_z^2 = -\frac{r}{<B>}\frac{d<B>}{dr} + F \qquad [8]$$

As previously stated, ν_z^2 is negative where the flutter is not sufficiently large to compensate for the defocusing due to the increase with radius of the isochronous field and axial defocusing is to be expected at small radii. Axial focusing can be successfully attained

in this central region from the first term in equation [8] by abandonment of isochronism if the ions do not get out of phase with the accelerating voltage.

The procedure used to determine the necessary average magnetic field to give axial focusing was as follows: (1) A $<B(r)>$ which would give a desirable axial focusing frequency was calculated from the smooth approximation. (2) The phase slip for a proton with a given energy gain per revolution was calculated; if it was greater than 90 degrees, this field was abandoned and a $<B(r)>$ with a less desirable ν_z was tried. It was assumed that the azimuthal variation of the magnetic field would not be changed by the alteration of $<B(r)>$.

The first trial $<B(r)>$ considered was the average field necessary to maintain ν_z at a constant value of 0.24 over the range of small radii where the sector focusing is weak. This field was constructed by a numerical integration of equation [8] by Simpson's 1/3 rule. The flutter shown in figure 3 was used. $<B(r)>$ was calculated by this method from r = 0.17 to r = 0.02 cyclotron units at radius increments of 0.01. The resultant average field and the isochronous field are shown in figure 5. After the first and second differences of this calculated field were smoothed, ν_z and the phase slip were obtained at successive energy values by use of the equilibrium orbit code. The results of this computer run showed that ν_z remained relatively constant at the desired value of 0.24 over the entire central

region of the field. However, the phase slip was excessive. Hand calculations showed that a proton with an energy gain per revolution of 0.28 mev would drop more than 90 degrees out of phase with the radio frequency accelerating voltage before it traversed 1/4 the radius of the magnetic field.

This average field was abandoned because of the unacceptable phase slip but valuable information was obtained from the computer run. As shown by Heyn and Khoe (3), if the non-isochronous and the isochronous fields are plotted as functions of the radius squared, the area between these curves is proportional to the cumulative phase slip. The area above the isochronous plot will correspond to negative phase slip and the area below to positive phase slip. This can be approximately understood by noting that the phase slip acquired by a particle during a given revolution is proportional to the difference between the field experienced by the particle and the isochronous field; and due to acceleration, the radius increase per revolution for the particle varies approximately as the square of the radius of its orbit. The phase slip of an ion is quite sensitive to the energy gain per revolution, for it is this which determines the number of revolutions that it will remain in a region where a given phase slip per turn is acquired. The phase slip as a function of radius can easily be calculated from the results of an equilibrium orbit code run if the energy gain per revolution is specified. Hence, the area corresponding to a

phase slip of, say, 20 degrees can be determined once a computer run is made with the equilibrium orbit code using a nonisochronous magnetic field. This was done for a proton with an energy gain per revolution of 280 kev using the average field shown in figure 5.

A second trial average magnetic field was numerically calculated with the general field shape suggested by Cohen and others (5, 3). At the center, this second field is made larger than the isochronous one and it falls off with increasing radius until it is well below the isochronous field, then increases more rapidly than the isochronous field at radii where the flutter is strong enough to give adequate focusing. The phase is thus shifted negative and back toward and perhaps through zero to a positive value.

With information obtained from the above mentioned orbit code run, the phase slip can be approximated accurately and quickly by graphical methods. The average field need only be calculated roughly from equation [8] since it was found from the results of the previous orbit code run that smoothing the first and second difference of $<B(r)>$ is sufficient to obtain a smooth ν_z as a function of radius plot.

The procedure for this numerical calculation was as follows: A field value, which was less than the corresponding isochronous field value, was chosen at a radius where the square root of the flutter equaled a desirable value for ν_z. The field to be calculated was assumed to go through a minimum at this point. The field at a

radius 0.01 cyclotron unit nearer the center was calculated from the following approximation of equation [8]

$$\nu_z^2(r_{i-1}) = -\frac{r_i + r_{i-1}}{B_i + B_{i-1}} \frac{B_{i-1} - B_i}{r_{i-1} - r_i} \frac{F(r_i) + F(r_{i-1})}{2}$$

or

$$B_{i-1} = \left[\frac{1 + \left(\nu_z^2(r_{i-1}) - \bar{F} \right) \frac{r_i - r_{i-1}}{r_i + r_{i-1}}}{1 - \left(\nu_z^2(r_{i-1}) - \bar{F} \right) \frac{r_i - r_{i-1}}{r_i + r_{i-1}}} \right] B_i \qquad [9]$$

where

$$\bar{F} = \frac{F(r_i) + F(r_{i-1})}{2}$$

The field value at each successive radius increment of $r = \pm .01$ was calculated from the previously determined field value. $\nu_z^2(r_{i-1})$ was used as an adjustable parameter to maintain the proper area between the calculated and the isochronous average magnetic fields. If ν_z could not be maintained as a slowly varying function of radius, the calculations were abandoned and another initial field value was chosen. The average field which resulted from these calculations is shown in figure 6.

The equilibrium orbit code was used to check the axial focusing frequency and the phase slip at successive energy values of $\Delta E = 280$ kev over the energy range where the average field deviates from isochronism. Figure 7 shows the plot of the axial focusing frequency which was obtained. The phase slip for a proton assumed to spend a

half revolution on successive equilibrium orbits of ΔE = 140 kev is shown in figure 8.

The axial focusing obtained from the radial dependence of the magnetic field is very good in the central region of the field. ν_z falls off only slightly at small radii to a value of 0.17, which occurs at the radius which corresponds to the equilibrium orbit of a 70 kev proton. The phase slip acquired is quite tolerable over this range of radius values and seems to diminish at larger radii.

The axial focusing is demonstrated in figure 9 which shows the z motion of a proton accelerated in this magnetic field with an energy gain per half revolution of $\frac{\Delta E}{2} \cos \phi$. The data for this plot were obtained from a computer run with the general orbit code. The initial conditions of the proton were: E_o = 70 kev, r = .0062, P_r = .00013, z_o = .00300, P_z = .00000, ΔE = 280 kev.

The maximum phase slip was found to be $\pm$ 18 degrees. This is in good agreement with ϕ shown in figure 8. Table I shows the good agreement between the ν_z obtained from the equilibrium orbit code and the ν_z of an accelerated proton which was computed from 1/2 wavelengths of the z motion shown in figure 9. ν_z is shown at energies which correspond to the maxima and minima of this plot.

The damping of the axial motion shown in figure 9 can be understood in light of an approximate solution to equation [6]. Assume that the z motion as a function of the azimuthal angle can be described by

$$\frac{d^2 z}{d\theta^2} + \nu_z^2 z = 0$$

where ν_z is a slowly varying function of θ. If ν_z^2 is positive as indicated by figure 7 the WKB approximation (10) gives

$$z = \frac{a}{\sqrt{\nu_z}} \cos\left[\int_{\theta_o}^{\theta} \nu_z \, d\theta + b\right]$$

where a and b are arbitrary constants.

This is the equation of a pseudo-harmonic oscillation with varying amplitude of $\frac{a}{\sqrt{\nu_z}}$ and varying instantaneous wavelength of

$$\lambda = \frac{2\pi}{\nu_z}$$

Hence the square of the amplitude as a function of the wavelength should plot a straight line. Figure 10 shows the good agreement between this approximation and the amplitude-wavelength relationship obtained graphically from figure 9.

Table 1

ν_z of an Accelerated and Nonaccelerated Protons

E mev	ν_z (figure 9)	ν_z (orbit code)
0.616	0.168	0.176330
1.101	0.186	0.186017
1.817	0.187	0.187869
2.361	0.187	0.188186
3.194	0.188	0.188815
7.822	0.2154	0.212180
8.215	0.2156	0.218960

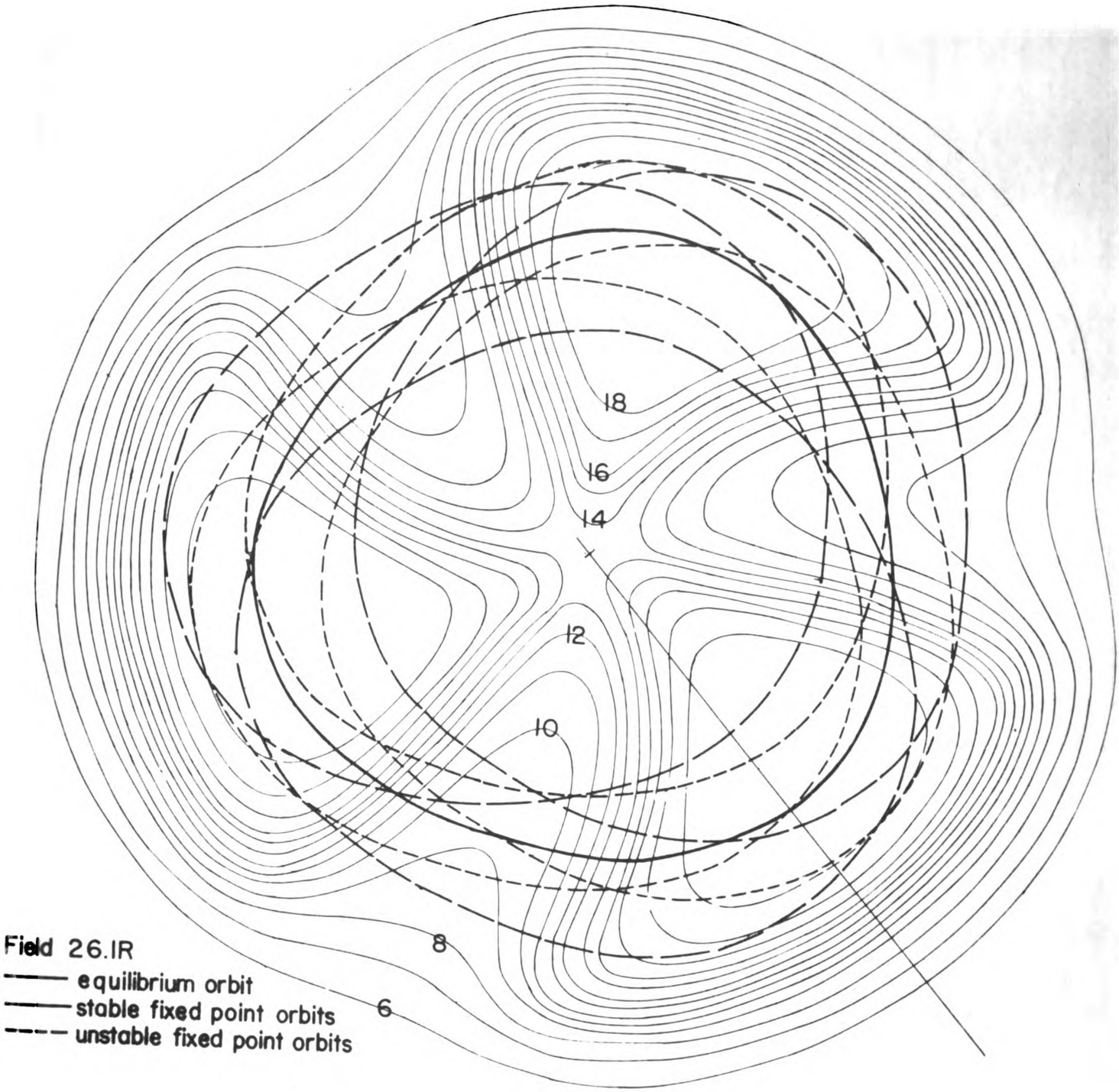

Figure 1. The magnetic field in the medial plane.

Equilibrium orbit of an ion in a three sector cyclotron

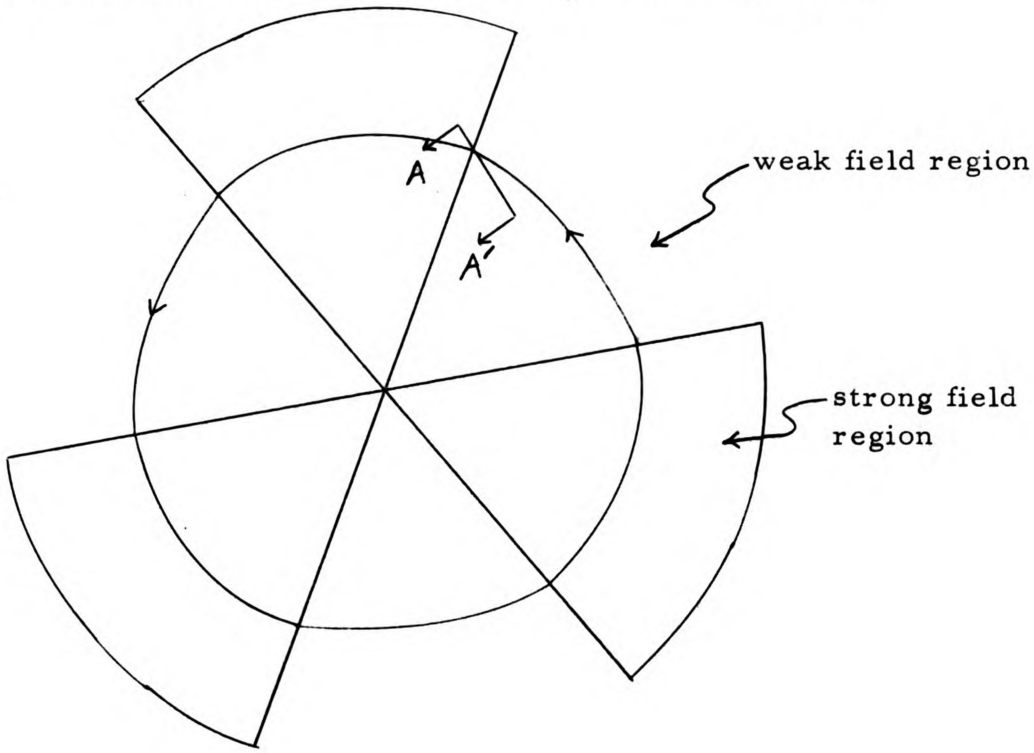

Magnetic field at edge of the wedge

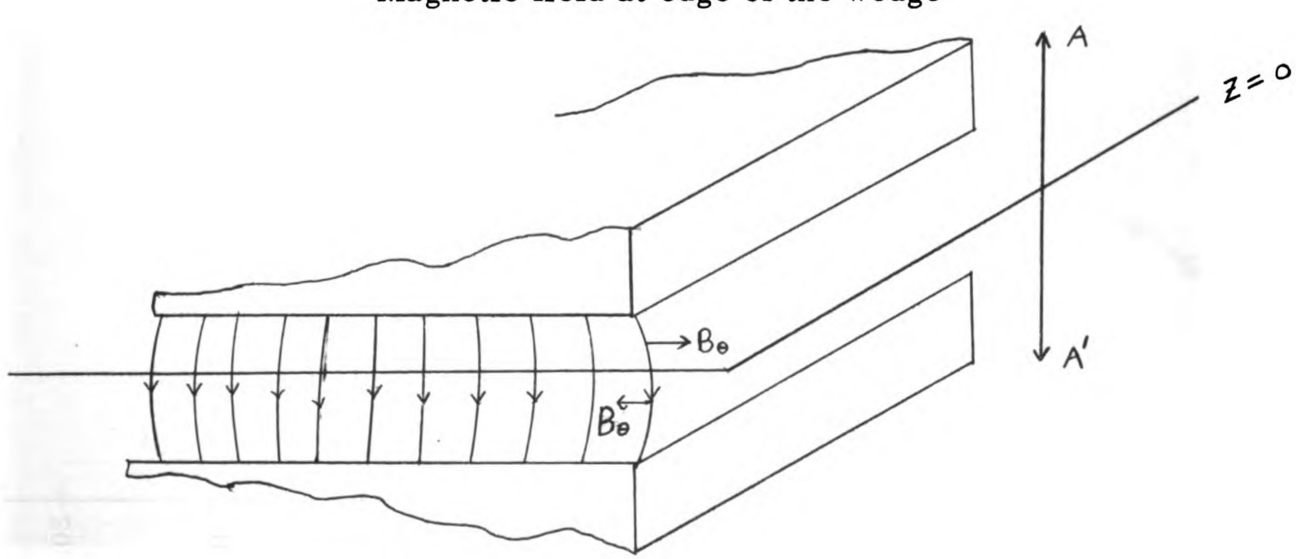

Figure 2. The axial focusing of a three sector magnetic field.

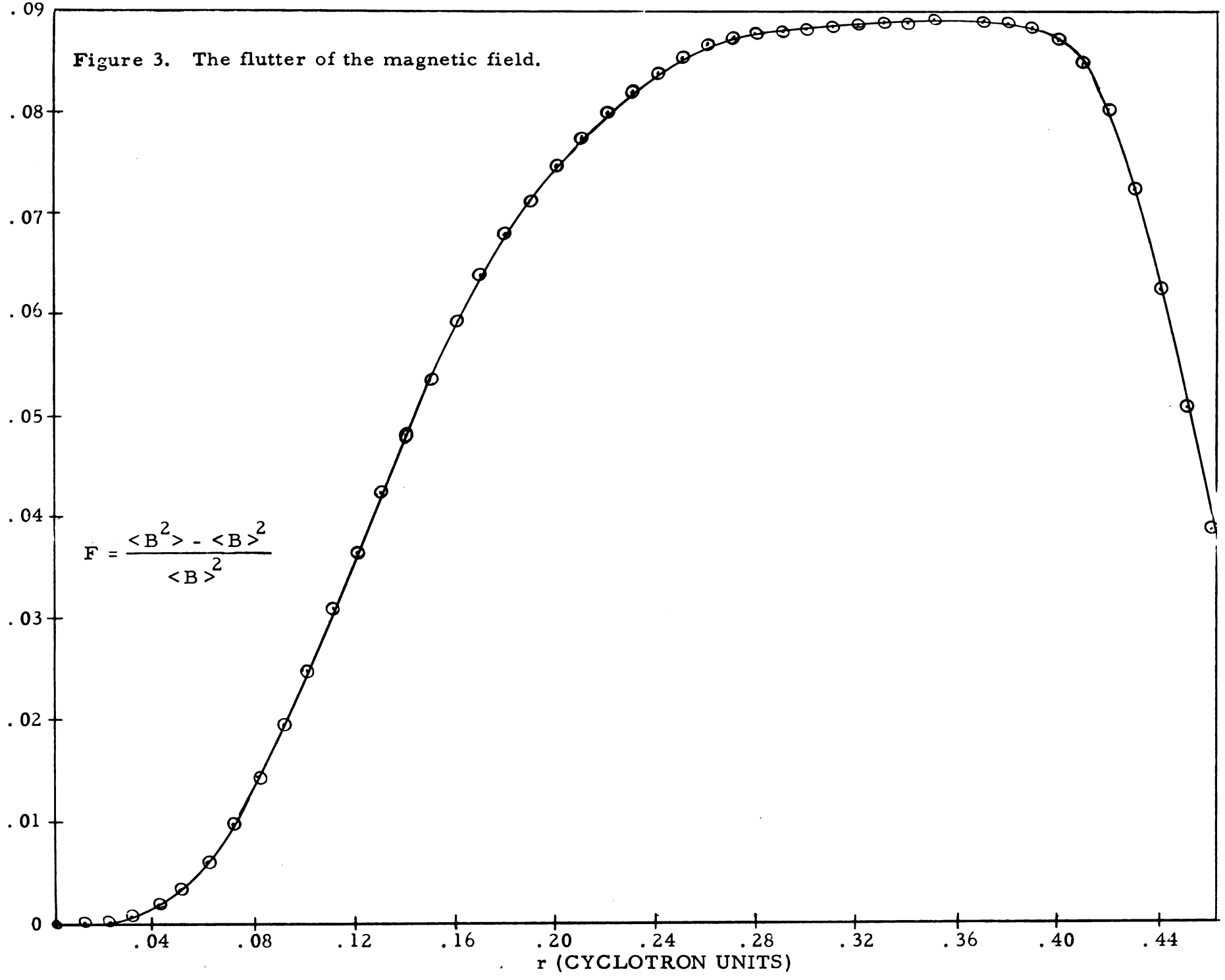

Figure 3. The flutter of the magnetic field.

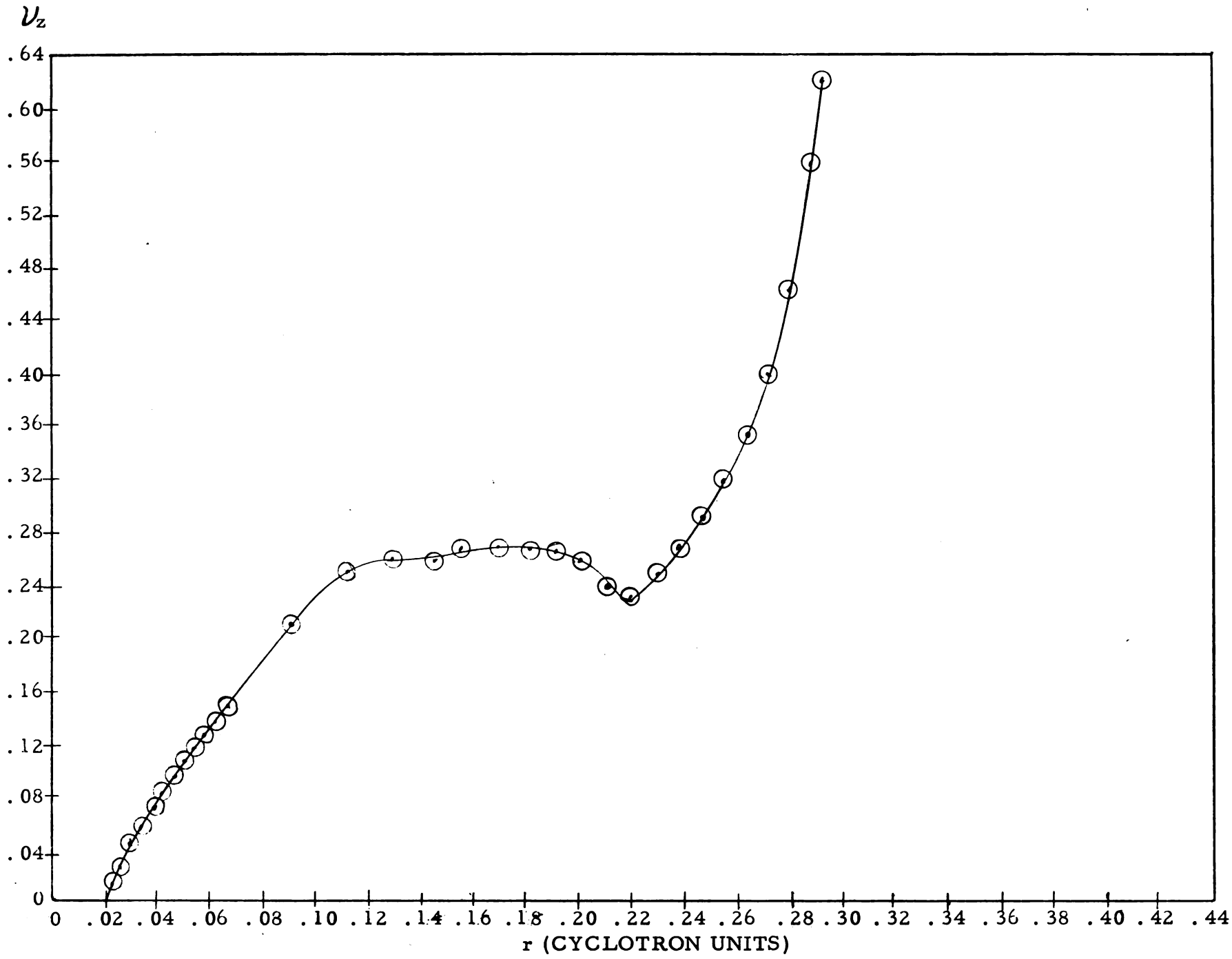

Figure 4. The axial focusing frequency of the isochronous magnetic field.

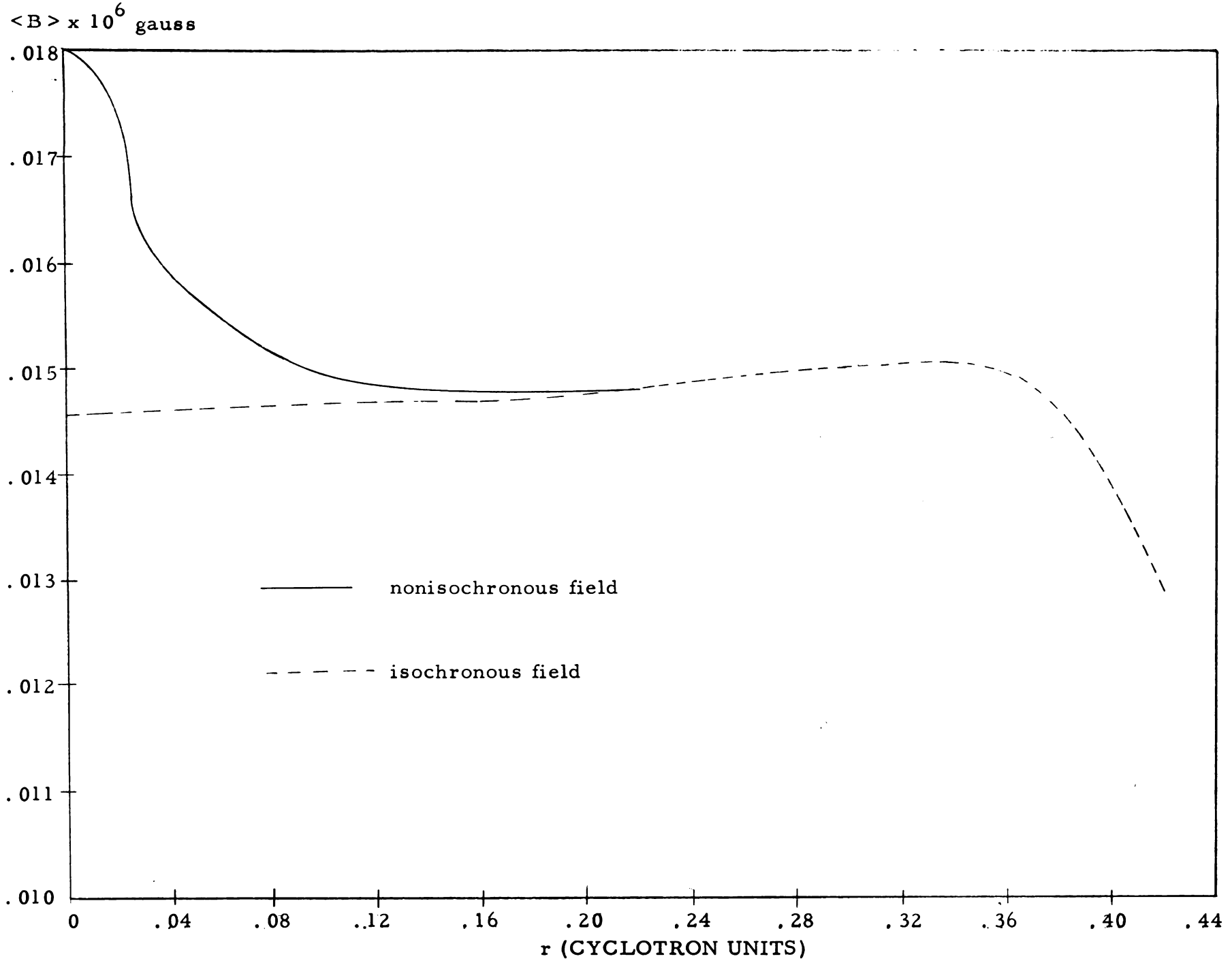

Figure 5. The average magnetic field necessary for a constant ν_z.

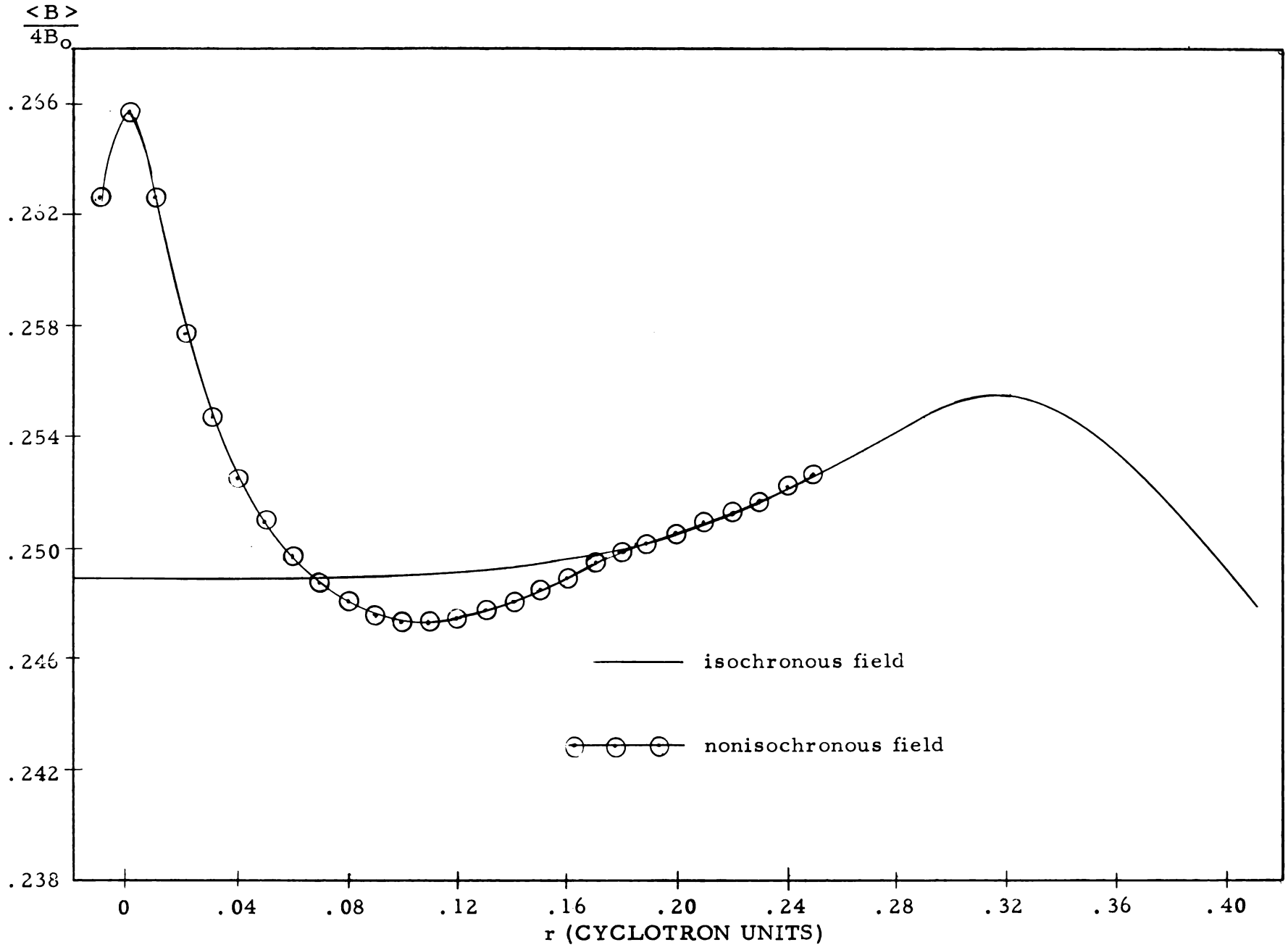

Figure 6. The nonisochronous average magnetic field with acceptable phase slip.

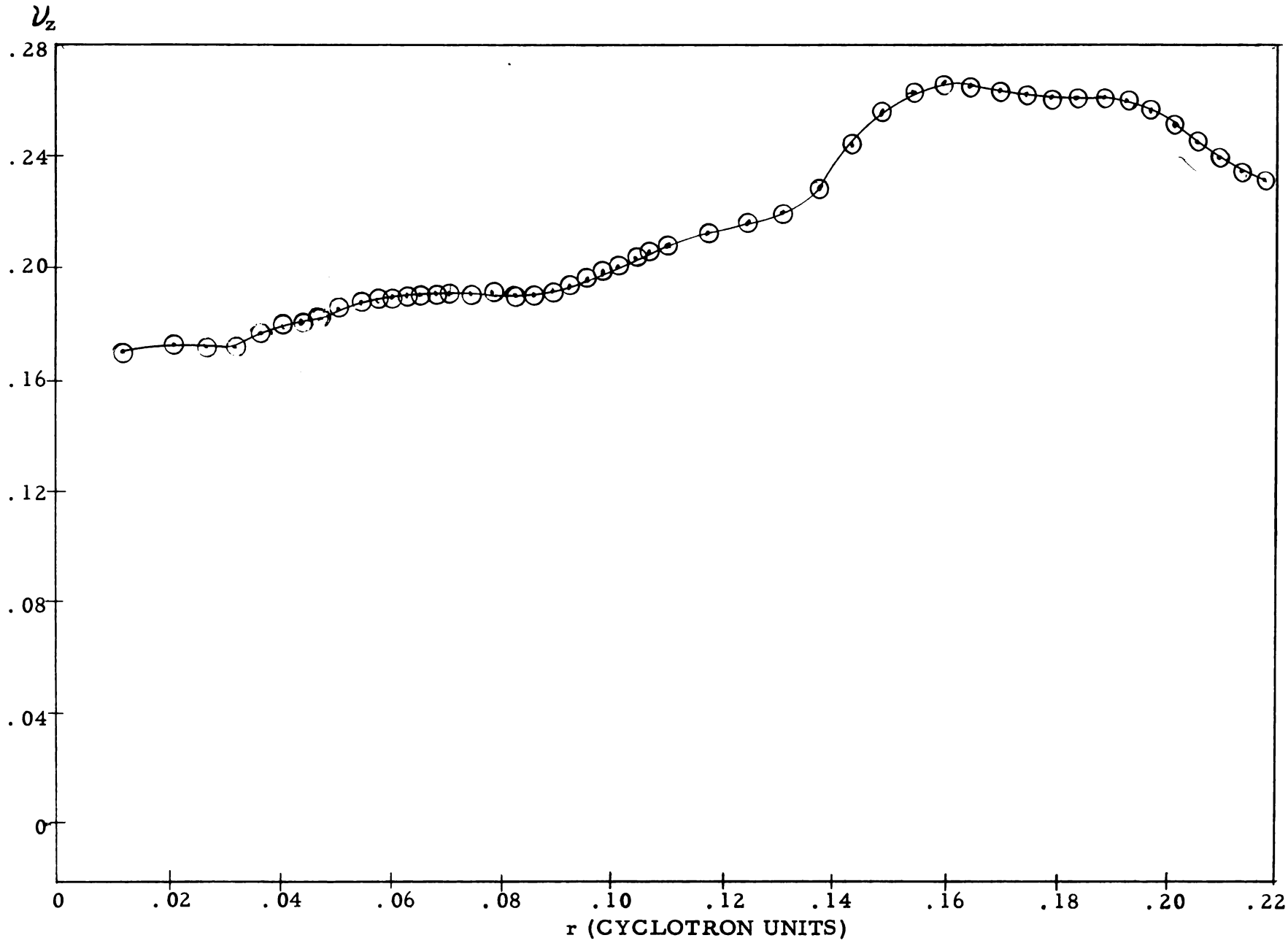

Figure 7. The axial focusing frequency of a proton in the nonisochronous field.

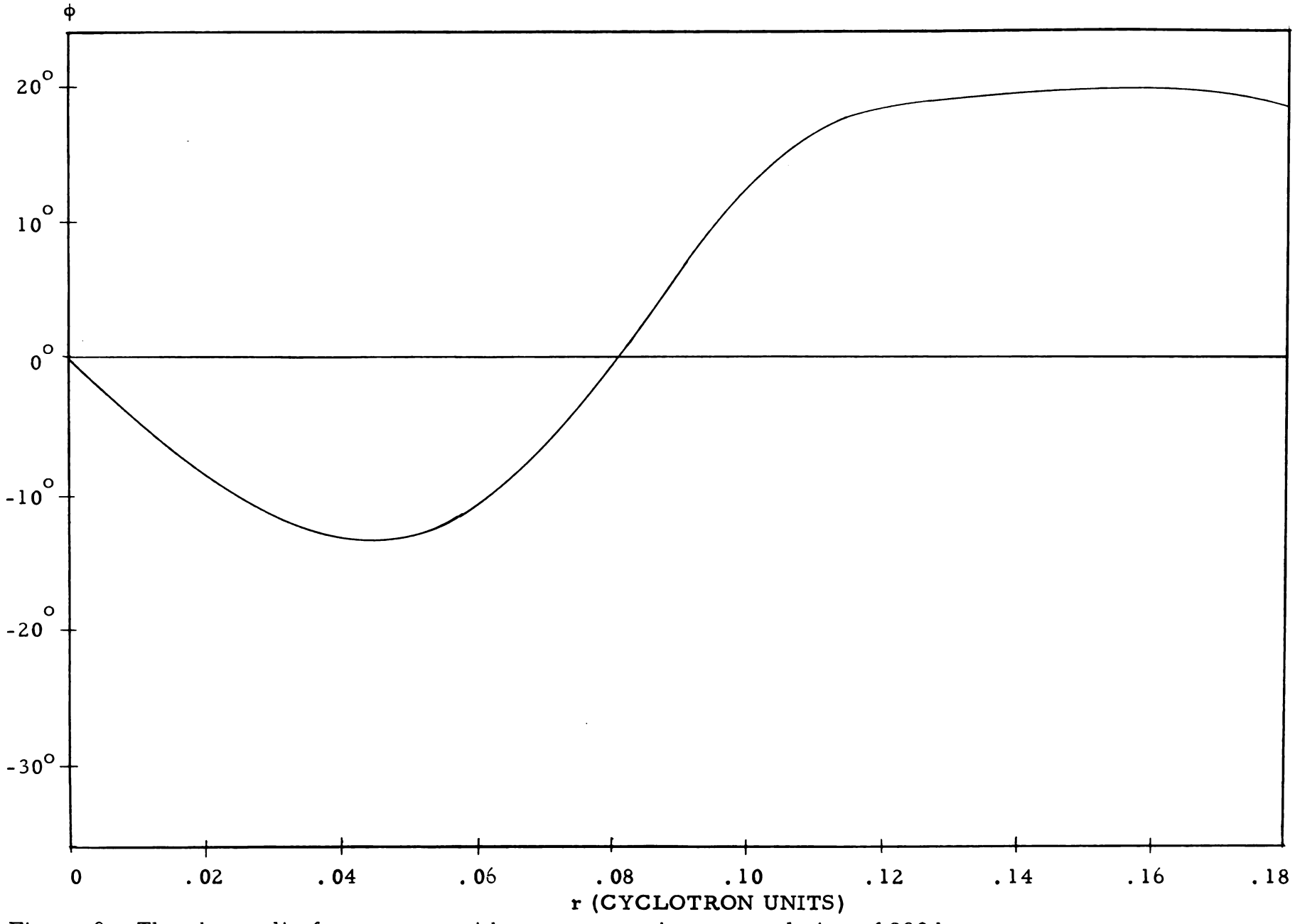

Figure 8. The phase slip for a proton with an energy gain per revolution of 280 kev.

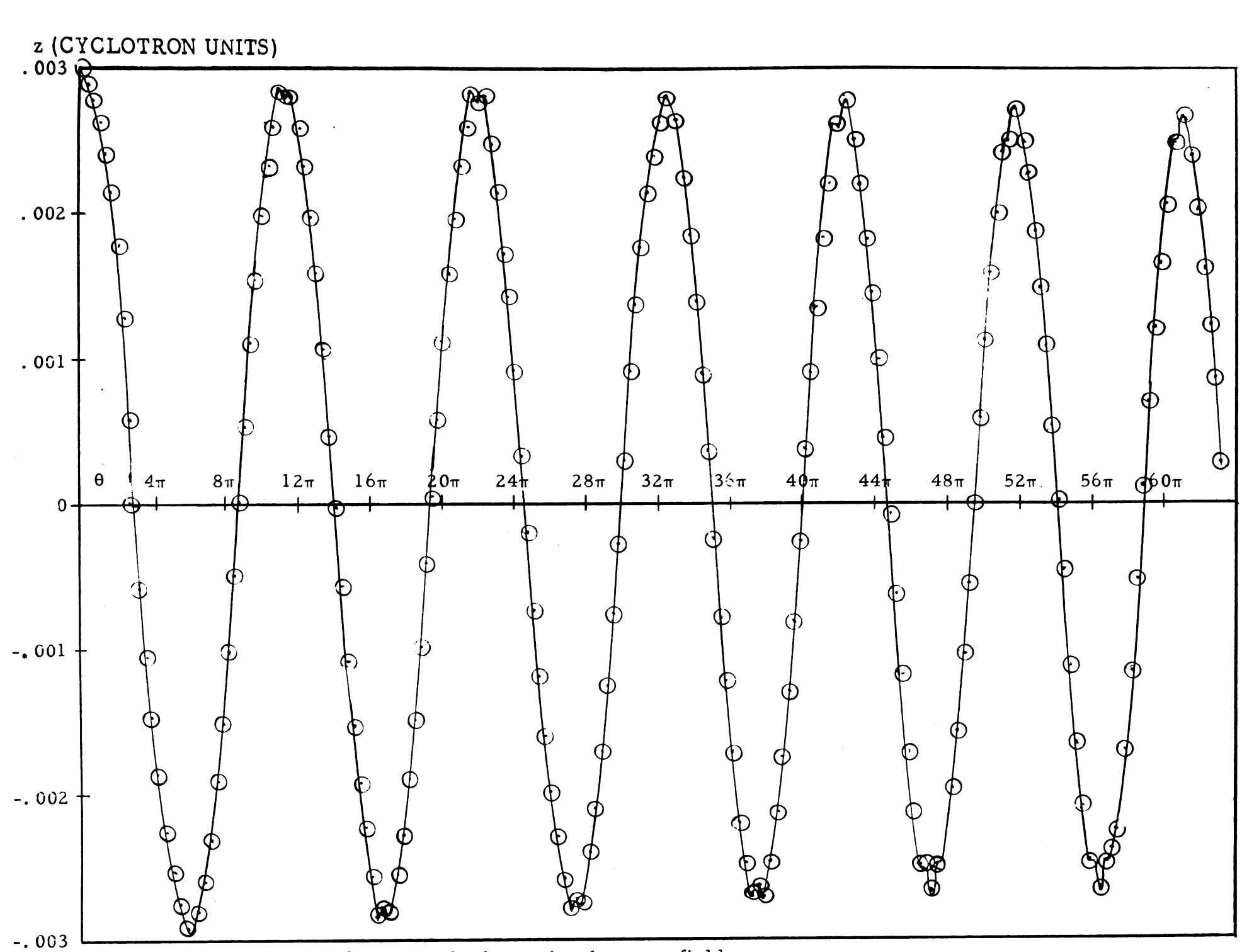

Figure 9. The axial motion of a proton in the nonisochronous field.

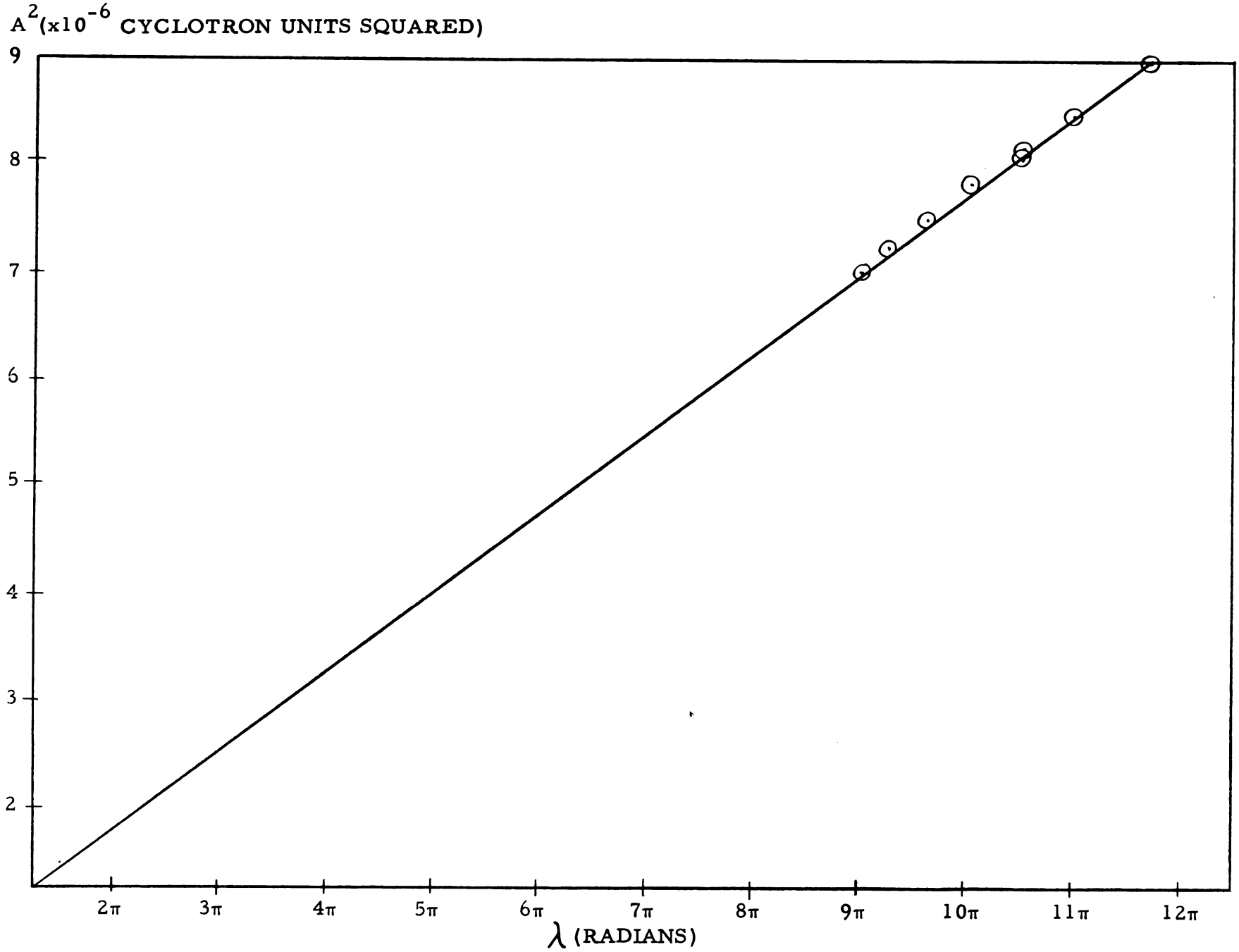

Figure 10. The amplitude damping of the axial motion.

SECTION II

RADIAL STABILITY AND RESONANCE TRAVERSAL

The feature which was so carefully built into the average magnetic field in Section I to give axial focusing introduces another problem; namely, that the ions must pass through a radial oscillation resonance near the center of the cyclotron (5). The radial oscillation frequency is given by the smooth approximation (6) as

$$\nu_r^2 = 1 + \frac{r}{\langle B \rangle} \frac{d\langle B \rangle}{dr} \qquad [10]$$

It is seen from equation [10] that ν_r is necessarily unity at r equals zero. However, if the ion source is situated between the dee gap in such a way that the ions are immediately accelerated to an energy of, say, 70 kev $\frac{d\langle B \rangle}{dr}$ is negative; then, in effect, ν_r increases from a value less than unity to become equal to unity when the average magnetic field changes from a decreasing to an increasing function of radius then continues to increase with radius. The radial oscillation frequency for a proton in the magnetic field under consideration was calculated by using the equilibrium orbit code and it is shown in figure 11.

$\nu_r = 1$ corresponds to a quadratic radial resonance in a three sector cyclotron. An approximate mathematical treatment of the traversal of 3/3 radial resonance by Sturrock (13) shows that a large fraction of the ions are lost if the beam of ions spends many revolutions

near this resonance. However, its effects may not be catastrophic, since accelerated ions spend only a small amount of time near the resonance. The effect of this resonance on a beam of ions must be carefully investigated before the method of achieving axial focusing described in Section I can be used.

The reason that a radial resonance is to be expected at ν_r equal unity can approximately be understood from a qualitative description of the trajectories of ions in the magnetic field plot shown in figure 1. First consider the effects of the radial variation in the magnetic field on the motion of an ion which initially has a small radial displacement from its equilibrium orbit. The radius of curvature of such an ion is given by

$$r = \frac{P}{e\langle B\rangle} \qquad [11]$$

where e and P are the ions charge and momentum, respectively and $\langle B \rangle$ is the average magnetic field along its trajectory. If the radial dependence of the magnetic field is such that ν_r^2, as given by equation [10], remains positive the ion will undergo radial oscillations about its equilibrium orbit. Differentiation of equation [11] shows that if the average magnetic field as a function of radius decreases less rapidly than $1/r$ radial instability is not to be expected from the radial variation in the magnetic field. The average magnetic field described in Section I satisfied this requirement for radial stability.

Since the radial oscillations of interest are those which have an oscillation frequency near unity, it is convenient to consider the

possible trajectories of ions in terms of this frequency. The resonance occurs at a radius approximately 1/7 the radius of the magnetic field plot shown in figure 1; hence the equilibrium orbit of an ion near resonance is almost circular and quite small in comparison to the dimension of the field. Consider the trajectory of an ion, near, but not at resonance, which initially has a small radial displacement from its equilibrium orbit. The trajectory after one revolution will also be almost circular with its center displaced. However, since ν_r is not unity the ion will reach its maximum radial displacement at a different azimuthal angle so that the orbit will not close. The azimuthal angle traversed by the ion before this maximum displacement occurs will be greater or less than 2π, depending on whether ν_r is greater or less than unity. After many revolutions the trajectory will form a rosette-shaped trace which is illustrated in figure 12. It follows that whether the trajectory for an ion which is revolving in a counterclockwise direction advances around the rosette in a counterclockwise or clockwise direction depends upon whether ν_r is greater or less than unity.

In the above discussion only the effect of the radial variation of the magnetic field was considered. The radial instability of the 3/3 resonance arises from the threefold symmetry of the azimuthal variation of the magnetic field. Hence, the effect of the azimuthal variation of the field on the rosette-shaped trajectory shown in figure 12 must be considered. Due to the threefold symmetry of the field

shown in figure 1, the equilibrium orbit is slightly triangular. This can be seen by consideration of equation [11]. The amplitude of the radial oscillations off this orbit will be enhanced or diminished during a given revolution by the azimuthal gradient of the field, depending on the azimuthal position at which the ion crosses the equilibrium orbit. If the radial oscillation frequency is not equal to unity, the rosette trajectory is maintained and the amplitude of oscillation is alternately enhanced and diminished. This gives radial stability for small amplitudes of oscillation near resonance. What is meant by small amplitudes will be shown shortly.

As ν_r approaches unity, many revolutions are required for a particle's trajectory to complete the rosette pattern. As a consequence, an ion with a ν_r nearly equal to unity will traverse the same azimuthal sector of the magnetic field for many consecutive revolutions. In doing so, it will experience the effect of a similar magnetic gradient during each revolution. Consider such an ion whose radial amplitude is increasing as it sweeps through an increasing magnetic gradient near one of the three magnetic "hills" shown in figure 1. If its radial amplitude is larger than a certain critical value, the amplitude will increase with each successive revolution. The trajectory of the ion will deviate from the rosette pattern and form a trochoid-shaped pattern, shown in figure 12, which will move radially outward in the field gradient of the hill, slowly at first then more rapidly. This is what is meant by radial instability. If, initially, the amplitude had

been smaller than the above mentioned critical value, it would require many revolutions before disastrously large amplitudes could build up and instead, the rosette shaped trajectory would carry the ion azimuthally out of this region of the field. As this ion progressed around the rosette, it would sweep through the decreasing field gradient on the other side of the hill, and its amplitude of oscillation would be decreased by the reversal of the above described process and radial stability would result. The limiting case between the stable and unstable trajectories occurs when the increase or decrease in radial amplitude introduced by the field gradient during one revolution is just large enough to compensate for the azimuthal shift of the trajectory so that the orbit is closed. This discussion is a simplification in that both the increase and decrease in amplitudes are enhanced by the gradient of the other two hills which the trajectory traverses each revolution. In summary; near resonance, the radial oscillations about the equilibtium orbit are stable if the initial amplitudes are smaller than a critical value, and unstable if they are initially larger than this critical value. If the initial amplitude is equal to this critical value closed orbits are formed. It follows from the above discussion that the magnitude of this critical amplitude depends upon the amount by which the particle is off resonance.

An analysis of the trajectories of ions in the central region of the magnetic field shown in figure 1 which have ν_r equal to unity shows

that any amplitude of oscillation about the equilibrium orbit will be unstable. All these trajectories will form trochoid shaped traces in the magnetic field gradient about the magnetic hills.

A useful procedure for investigating radial stability is the use of phase plots. If x, the radial displacement from the equilibrium orbit, and the conjugate momentum, $p_x = \frac{dx}{d\theta}$, are known, the center of curvature of the ion is defined. From geometrical considerations it can be seen that if p_x is plotted as a function of x, once per revolution, the resultant phase plot corresponds to the movement of the center of curvature of the trajectory at that azimuth angle. These phase plots can be used directly to gauge the range of radial oscillation amplitude for which the orbits are stable. It is easily seen that curves in phase space which close about the equilibrium orbit point correspond to the stable rosette shaped trajectories described earlier. The open curves correspond to the trochoid shaped trajectories of the unstable orbits.

A typical phase plane diagram (13) for an ion near resonance in a three sector magnetic field is shown in figure 10. The feature of interest is the triangular shape of the stable region which is defined by the three "unstable fixed point" labeled U. These points not only mark the boundary separating the stable and unstable region in the phase diagram, but behave in a manner analogous to that of the central equilibrium orbit, in that a particle starting at such a point on each successive revolution comes back to the initial point (14). Hence, they correspond to the limiting case between the rosette and trochoid

trajectories discussed earlier in this section.

As an ion is accelerated through resonance, the size of the stable region in phase space decreases to zero, and then steadily increases. Approximate behavior of particles accelerated through resonance can be inferred if the location of the unstable fixed points are known for successive energy values above and below resonance. For example, the number of revolutions required for ions with a given energy gain per turn to traverse the region of resonance effects can be determined. The effective size of the stability region can be found. The coordinates, in phase space, of the unstable fixed points were found by use of the orbit codes. The stable triangles are shown at energy increments of 0.25 mev in figure 14. The energy corresponding to resonance is 1.47 mev. The azimuthal angle in the field was chosen to correspond to the first dee gap crossing, for convenience. To view the effects of resonance traversal, consider a beam of protons in this magnetic field with an energy gain per revolution of 280 kev which were emitted from an ion source situated at the center of the cyclotron between the dee gaps. After two complete revolutions, the beam of ion will reach an energy of .50 mev. At this time the beam can be considered to be a spot in phase of, say, 0.003 cyclotron units in diameter which is located near the center of the large stable triangle. Three revolutions later, the stable region has decreased in size, leaving part of the beam in the unstable region where the amplitudes of the radial oscillations increase. The stable region continues to decrease in area, ceases

to exist at resonance, and then begins to expand. It is hoped that this expansion of the stable triangle will overtake the beam before excessive increases in the amplitudes occur.

The rate of expansion of the radial amplitudes while the beam is in the unstable region is determined from phase plots obtained by use of the general orbit code. Figure 15 is a phase plot at an energy of 1.25 mev, which is approximately one revolution below the resonance energy. The full radial scale of this graph is 4.52 inches. The stable region at this energy has decreased from 1.5 inches at 0.50 mev to 0.32 inches. Six orbits are shown; three within the stable region and three in the unstable region where the radial amplitude expansion occurs.

At Oak Ridge (5) and MSU (17), sufficient phase plots have been made for azimuthally variation magnetic fields of the type considered here, so that it is assumed that plots in the stable region will close about the equilibrium orbit point. These orbits were abandoned to conserve computer time since the number of revolutions required for the plot to close is approximately $\left|\frac{1}{\nu_r - 1}\right|$, which is 342 revolutions at this energy.

In the unstable region, amplitudes of the radial oscillation about the equilibrium orbit increase each revolution as indicated by the movement of phase points along the "outflowing asymptotes." This corresponds to the formation of the trochoid-like trajectories.

It can be noted from figure 15 that a particle near one of the unstable points in this region will move out radially, slowly at first, then more rapidly with each successive revolution. The rate of amplitude growth then depends upon the location of the orbits in phase space with respect to the unstable fixed points and upon the number of revolutions during which the particles have been in the unstable region.

Consider the motion of a proton, with an energy of 1.25 mev, which is displaced 0.7 inches from the equilibrium orbit along the outflowing asymptote in figure 15. After ten revolutions, its radial amplitude has increased to 2 inches; but, if its energy gain per revolution is 0.28 mev, in ten revolutions the proton will obtain an energy of 4.0 mev. Its amplitude stability limit would then be greater than 2 inches. Therefore, 1.25 mev protons with radial amplitudes less than 0.7 inches will probably survive the resonance traversal. The "effective" stable amplitude limit will actually be larger, since only a minority of the ions with this amplitude will have such unfavorable coordinates with respect to the unstable fixed points. Phase points of protons which have initial conditions that exceed the effective stable amplitude limit will not be overtaken by the expanding stable region. Such particles are said to fail to survive the resonance traversal. The conclusions obtained from this consideration are very encouraging, since the radial amplitudes are not expected to exceed 0.35 inches at this energy.

The investigation of radial stability thus far has been inferred by means of static phase plots and knowledge of the size of the stable region at energy values of interest. However, the problem of radial stability can only be completely settled by tracking the phase points of groups of ions as they are accelerated through resonance to an energy where the amplitude stability limit is quite large. The procedure for doing this is discussed in detail in the next section. It will be shown that an acceptably large central beam will survive the traversal of the 3/3 radial resonance in this magnetic field.

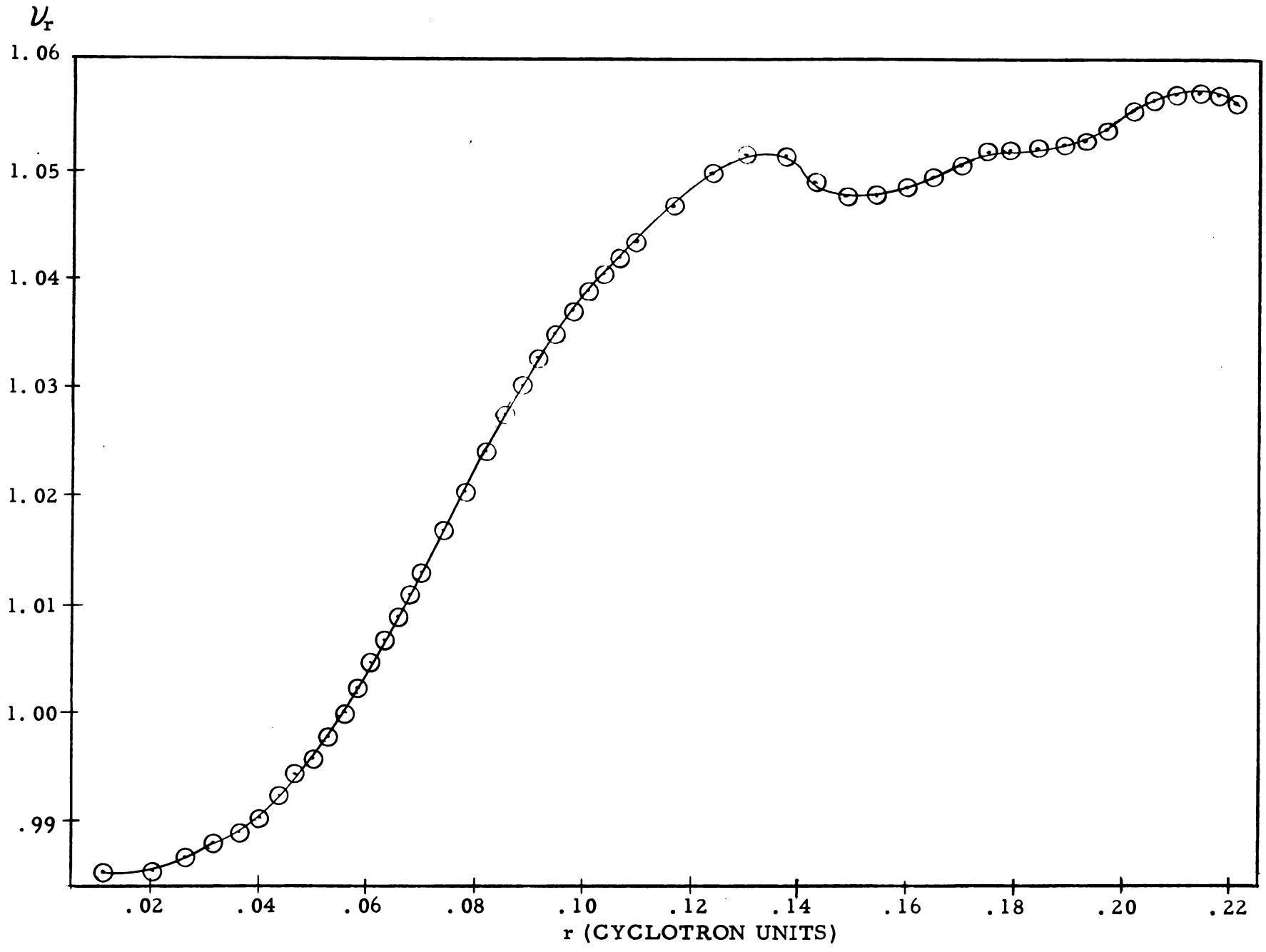

Figure 11. The radial oscillation frequency of a proton in the nonisochronous magnetic field.

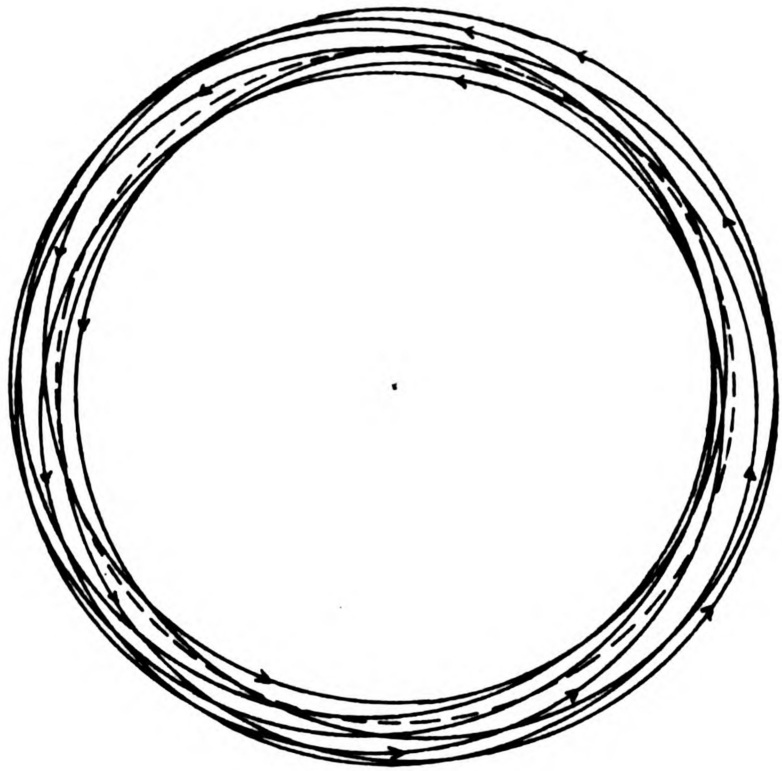

The rosette-shaped trajectory of stable radial oscillation

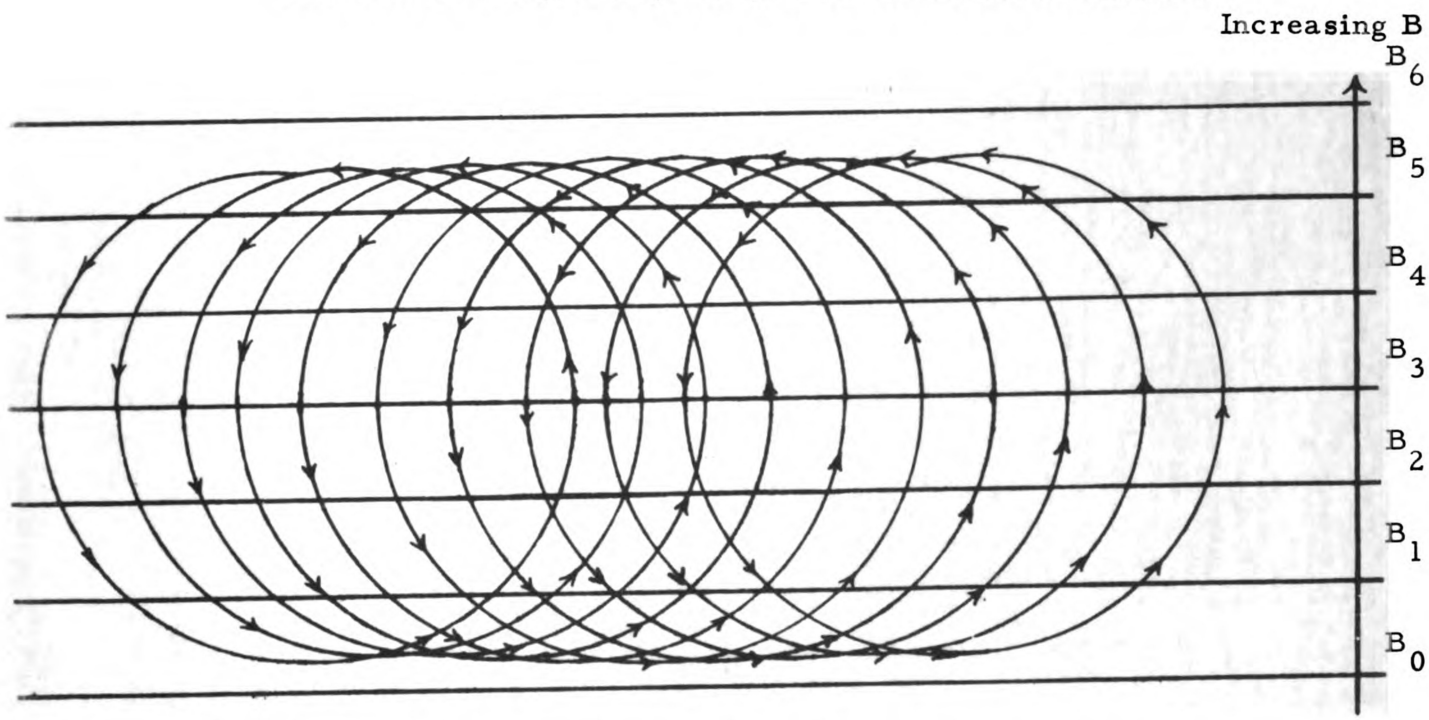

The trochoid-shaped trajectory of unstable radial oscillation

Figure 12. The stable and unstable trajectories in the median plane.

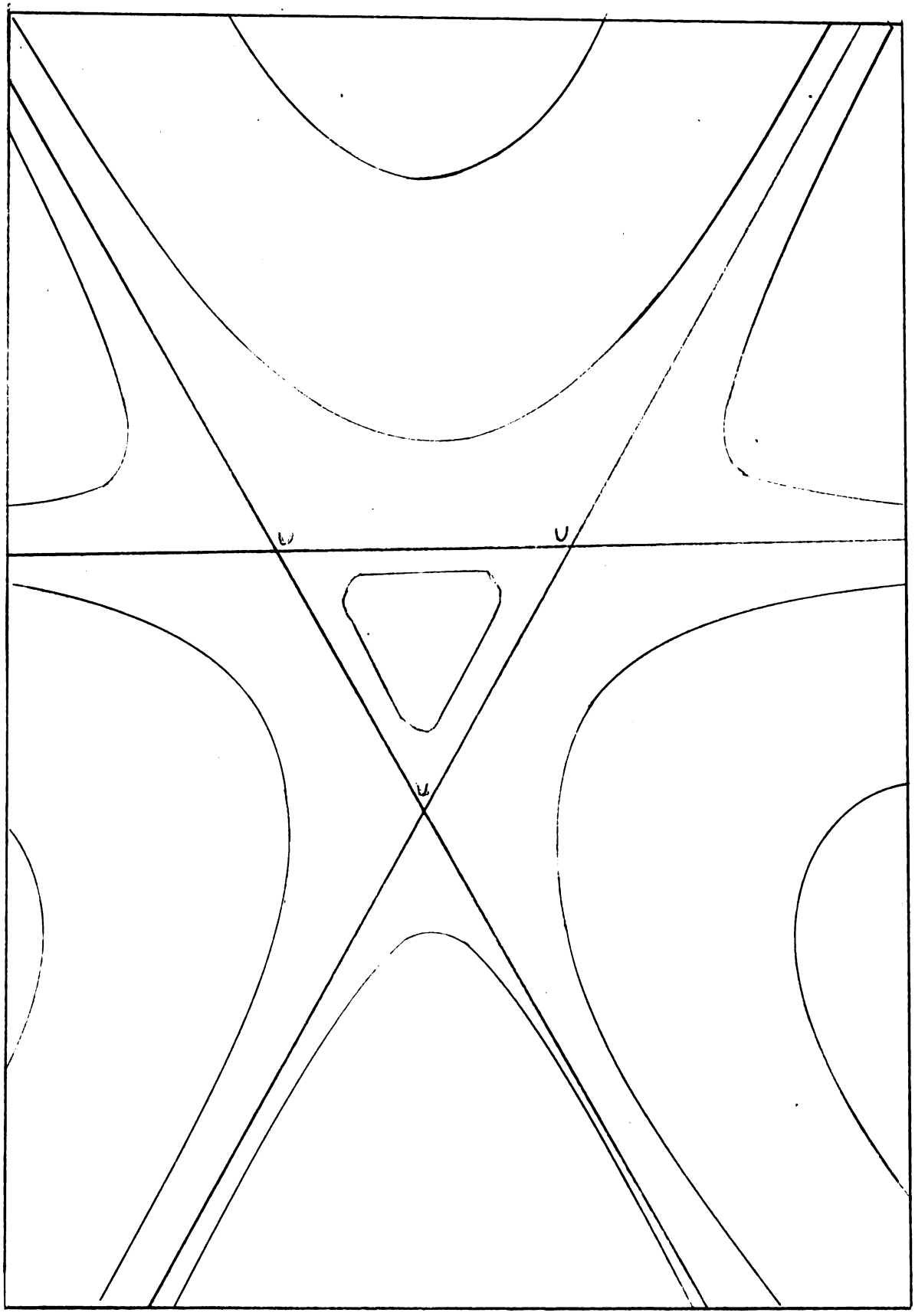

Figure 13. A phase diagram near resonance for a three sector magnetic field.

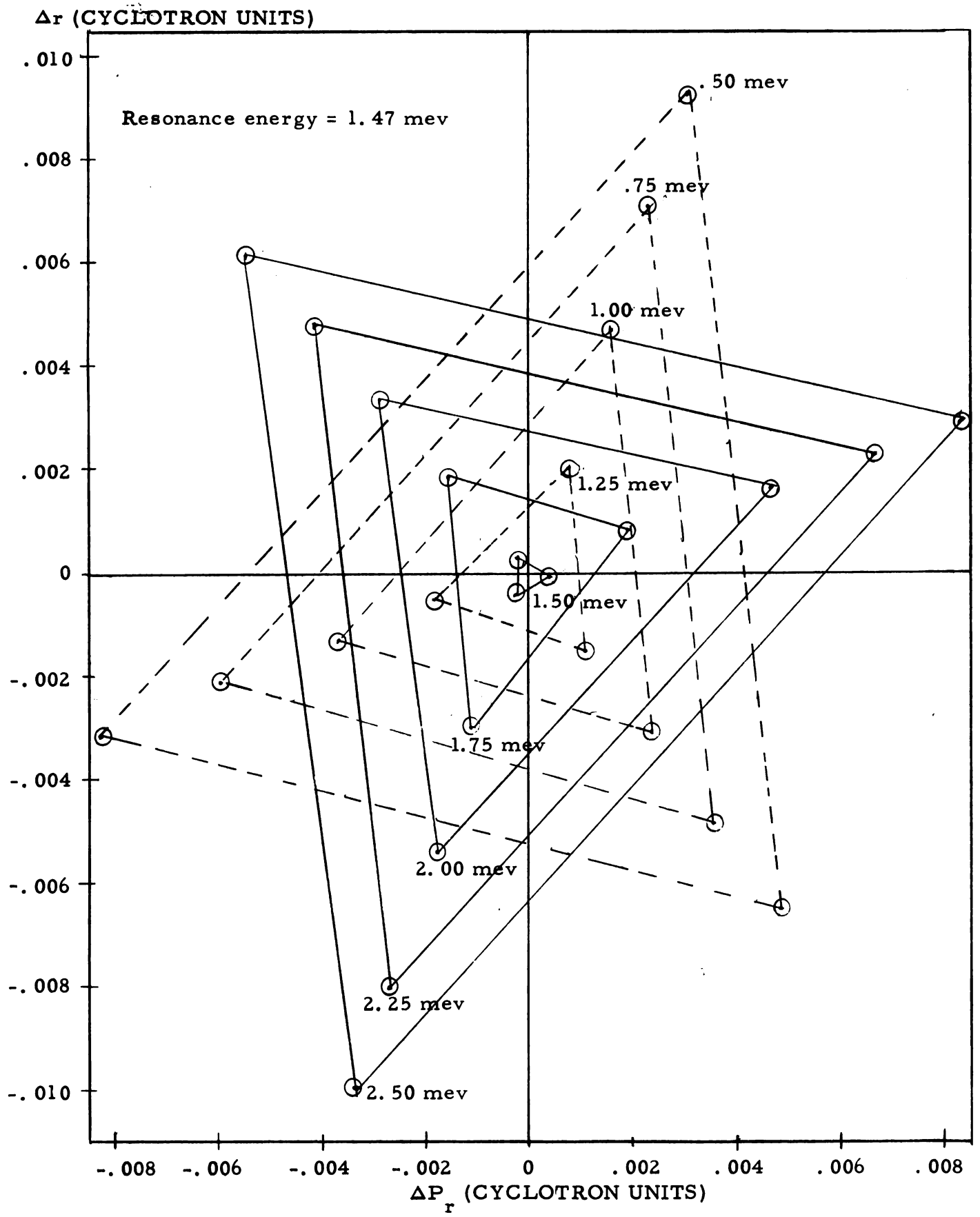

Figure 14. The stable regions at energies near resonance.

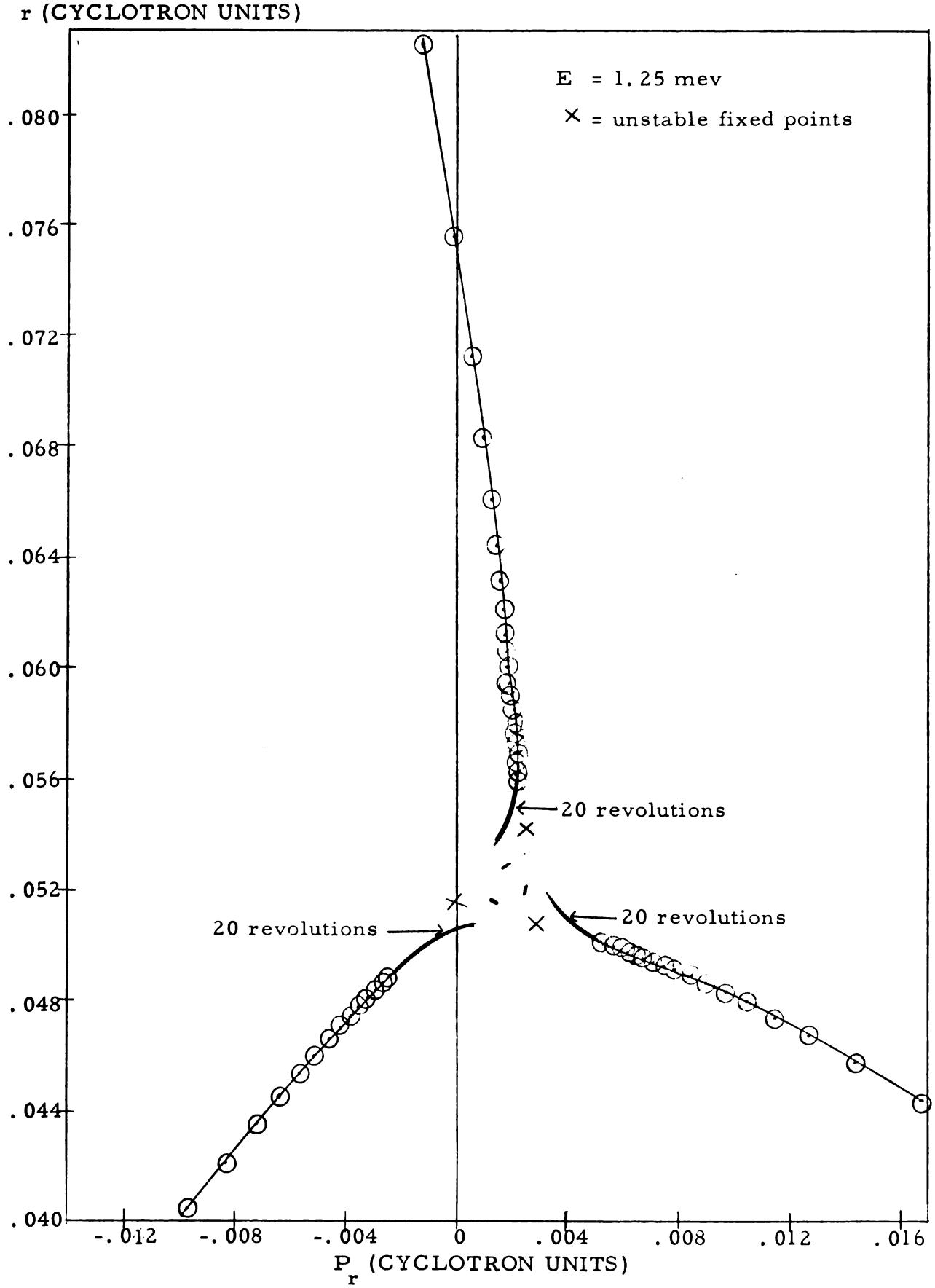

Figure 15. A phase plot 220 kev below resonance.

SECTION III

BEAM DISTORTION

In Section I it was stated that the general orbit code was used to simulate the acceleration of a proton from an initial energy of 70 kev to 9 mev. The radial orbital properties obtained from this computer run indicated that this particle survived the traversal of the 3/3 radial resonance. However, the survival of one ion means very little. It is the survival of a beam of ions with a minimal amount of distortion that is necessary for the efficient operation of a cyclotron. To investigate the feasibility of resonance traversal, a group of particles must be accelerated through resonance. It follows from Liouville's theorem (15) that the area enclosed in phase space must remain invariant during the acceleration process. Therefore, if the area in phase space enclosed by this group of particles is the size of the desired particle beam, the effect of resonance traversal on the entire beam can be predicted.

If four particles whose initial r and P_r values form a square in phase space are accelerated through resonance, the final phase area enclosed, although equal to the initial area, may be very distorted in shape. A beam of particles initially inscribed within this phase area would likewise be distorted.

The reason that beam distortion is to be expected can be understood by a consideration of the phase plot, shown in figure 15, and the

relative sizes of the stable regions at various energy values, shown in figure 14. Assume that initially the phase area, at an energy below resonance, is bounded by particles whose initial conditions do not exceed the effective stable amplitude limit discussed in Section II. The shape of the phase area will be unchanged as long as all the particles remain in the stable area. As these particles are accelerated, the stable region decreases in size, leaving the particles in the unstable region where their amplitudes of oscillation either increase or decrease. This change in radial amplitude corresponds to movements in various directions of the phase points along the flow lines shown in figure 15. The direction and rate of this movement will depend on the coordinates of the phase points with respect to the unstable fixed points and the number of revolutions that the particles remain in the unstable region. This will obviously change the shape of the phase area since its size is invariant. As the particles are accelerated, the resonance is traversed and the expanding stable region overtakes the points so that the distortion of the area ceases.

The distortion of the area can be very severe, since phase points with less favorable location with respect to the unstable fixed points move more rapidly, and hence remain outside the stable region for a greater number of revolutions. Obviously, the larger or less compact the initial phase area, the more severe the distortion.

For another view of the effects of beam distortion, consider a group of phase points enclosing a circle in the stable region at an

energy well below resonance. If, after resonance traversal, the area is distorted into a long, narrow shape, a much larger stable region at energies above resonance will be required to retain the phase points.

With these general principles in mind, the technique for investigating beam distortion can be understood in light of the relative sizes of the stable region shown in figure 14. If an ion is accelerated from the center of the cyclotron and reaches an energy of, say, 4 mev with r and P_r coordinates which lie within the stable region at that energy, the orbit thereafter will be stable (5). Also if a 4 mev ion initially on the equilibrium orbit at that energy is decelerated and traced to near zero energy its phase coordinates will locate the position of the ion source. In particular, if a group of ions with initial conditions that enclose an area in phase near the resonance energy equilibrium orbit phase point are accelerated to 4 mev and decelerated to near zero energy the proper location of the ion source can be found and the distortion of the central rays of the ion beam can be investigated.

The general orbit code can be adapted to investigate beam distortion and to determine the necessary initial conditions for the central ray of the ion beam. A slight modification of this code will simulate acceleration by increasing an ion's energy by a constant amount each half revolution. Hence, groups of particles with different initial r and P_r values will have a constant energy gain per revolution regardless of their respective phase slip. Also, deceleration of particles can be simulated by a similar procedure.

The distortion of the central rays of the particle beam was investigated by using the general orbit code to track a group of five protons with an energy gain per revolution of 280 kev from the resonance energy of 1.47 mev to a final energy of 3.99 mev and backward from resonance to 70 kev. The initial phase coordinates of the protons were chosen to form a 0.0028 cyclotron unit square, with one proton at the center, near the equilibrium orbit corresponding to resonance energy. The phase space coordinates were obtained for each particle at the end of successive revolutions. This computer run was then repeated for a proton initially at the center of this square with an axial displacement of 0.005 cyclotron units, to investigate possible coupling of the radial and axial oscillation by the "sum" or "difference" resonance.(16).

The results of these computer runs are shown in figure 16. It is seen that the shape of the square is only slightly distorted by the effects of resonance traversal. It was found that the maximum effects introduced into the phase coordinates of the central proton by including axial motion was less than 0.0006 cyclotron units. These results are very encouraging, in that the radial width of a beam enclosed by this phase area is 0.27 inches and the distortion is certainly tolerable. The feasibility of 3/3 radial resonance traversal for a sizable beam of protons is thus established.

It is desirable to know the dimensions of the region in phase space from which 70 kev protons can be accelerated without severe

beam distortion. This is accomplished by simulating the acceleration and deceleration of protons, with the array of initial r and P_r values shown in figure 17, in the manner described above. These phase points can be considered to form annuluses of various sizes and with different orientations with respect to the equilibrium orbit phase point. By tracking this array of phase points, the distortion of various parts of a large proton beam can be determined. As can be seen from figure 17, these phase points are symmetrically located with respect to the initial conditions of the five protons with radial displacement of .004, .006 and .010 cyclotron units. The array is slightly off center with respect to the phase coordinates of the equilibrium orbit corresponding to this energy, due to a computer error.

The distortion of this array of phase points during the acceleration process is shown at the end of the third, fifth, seventh and ninth revolutions in figures 18 through 22, respectively. The stable region and equilibrium orbit coordinates are also shown. The full scale of the radial axis is 5.42 inches on these plots.

From these graphs, it is seen that the distortion of the phase areas in the third and fourth quadrants is relatively slight, whereas it is very severe in the first and second quadrants. The reason for this can be seen by considering figure 18 in light of the static phase plots discussed in Section II. All but two of the particles in the third and fourth quadrants are in the stable region after two revolutions. These two particles have favorable phase space coordinates with respect to

the unstable fixed points, so that in a static phase plot their phase points would move parallel to the side of the stable triangle. These points are overtaken by the expanding stable region within two more revolutions and the distortion ceases.

The phase points in the first and second quadrants are more unfavorably located with respect to the unstable fixed points, and hence are moving more rapidly. It is seen that the distortion is very severe and that those particles with the largest radial values will not survive the resonance traversal.

The results of the computer runs simulating deceleration of these particles are shown in figures 22, 23, and 24. The distortion is less severe in this case since only five revolutions are required. The computer runs for the phase points in the third and fourth quadrants were not made since it can be safely assumed that distortion would be less in that region. The justification of this assumption can be seen in figures 22 and 23, since the phase points in question would have been nearer the equilibrium orbit phase point, hence less distorted than the corresponding first and second quadrant points. All the third and fourth quadrant phase points would have been in or very near the stable region in figure 23.

At 70 kev, the distortion is again severe in the second quadrant but is less severe in the first quadrant. The stable region is not shown in figure 22, but as shown in the appendix it is approximately the full scale of the graph.

The results shown in figures 17 through 24 indicate that there exists an area in phase space at 70 kev of perhaps . 006 x . 006 cyclotron units from which a beam of protons can be accelerated with an energy gain per revolution of 280 kev without severe beam distortion. This area is centered near but above the equilibrium orbit phase point in figure 24. The distortion of the beam is diminished as the central region of this area is approached. In summary, all particles in a 0. 70 inch beam of protons with an energy gain of 280 kev per revolution would very likely survive the 3/ 3 radial resonance traversal. A beam composed of these protons, whose radial displacements are a half inch or less, would not be severely distorted.

The data given in figures 16 through 24 were obtained by use of a modification of the general orbit code which assumes a square wave acceleration voltage. In an actual case both the phase slip and the spread in phase of particles must be taken into account. The phase slip as a function of radius is shown in figure 8. It can be seen that a sinusoidal voltage would never be farther than 15 degrees from its peak when particles cross the dee gap. The maximum phase spread at successive dee gap crossings for the deceleration run shown in figure 16 is given in table II. From these data it is seen that the square wave assumption is good and that the use of a sinusoidal voltage would not significantly change the results.

Table II

Phase Slip Spread for the Deceleration Run Shown in Figure 14

E mev	$\Delta\phi$ (max.)
1.33	5.3°
1.19	4.1°
1.05	7.4°
0.91	8.2°
0.77	8.7°
0.63	2.0°
0.49	11.5°
0.33	7.7°
0.21	14.4°
0.07	8.7°

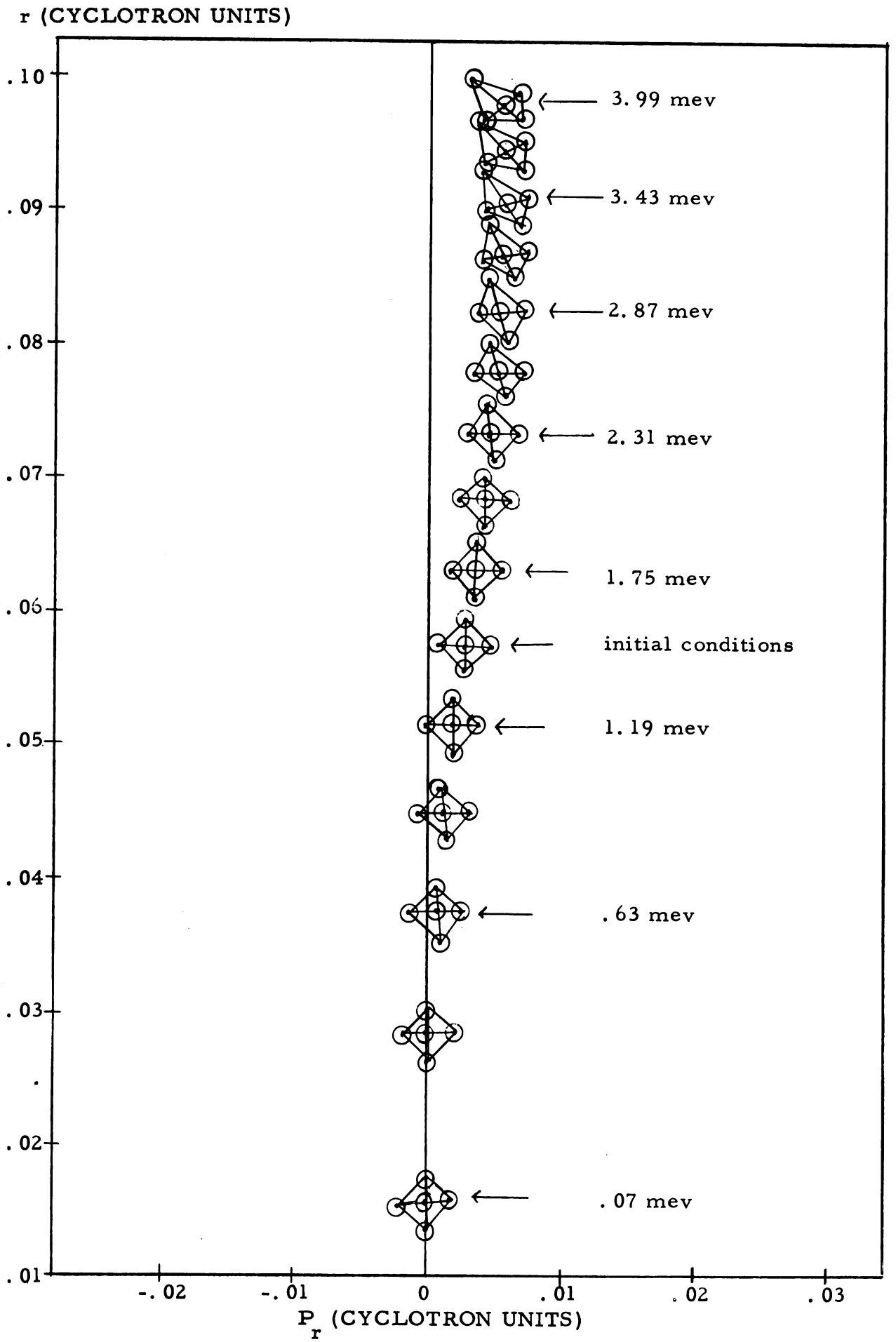

Figure 16. The distortion of a 0.27 inch central beam.

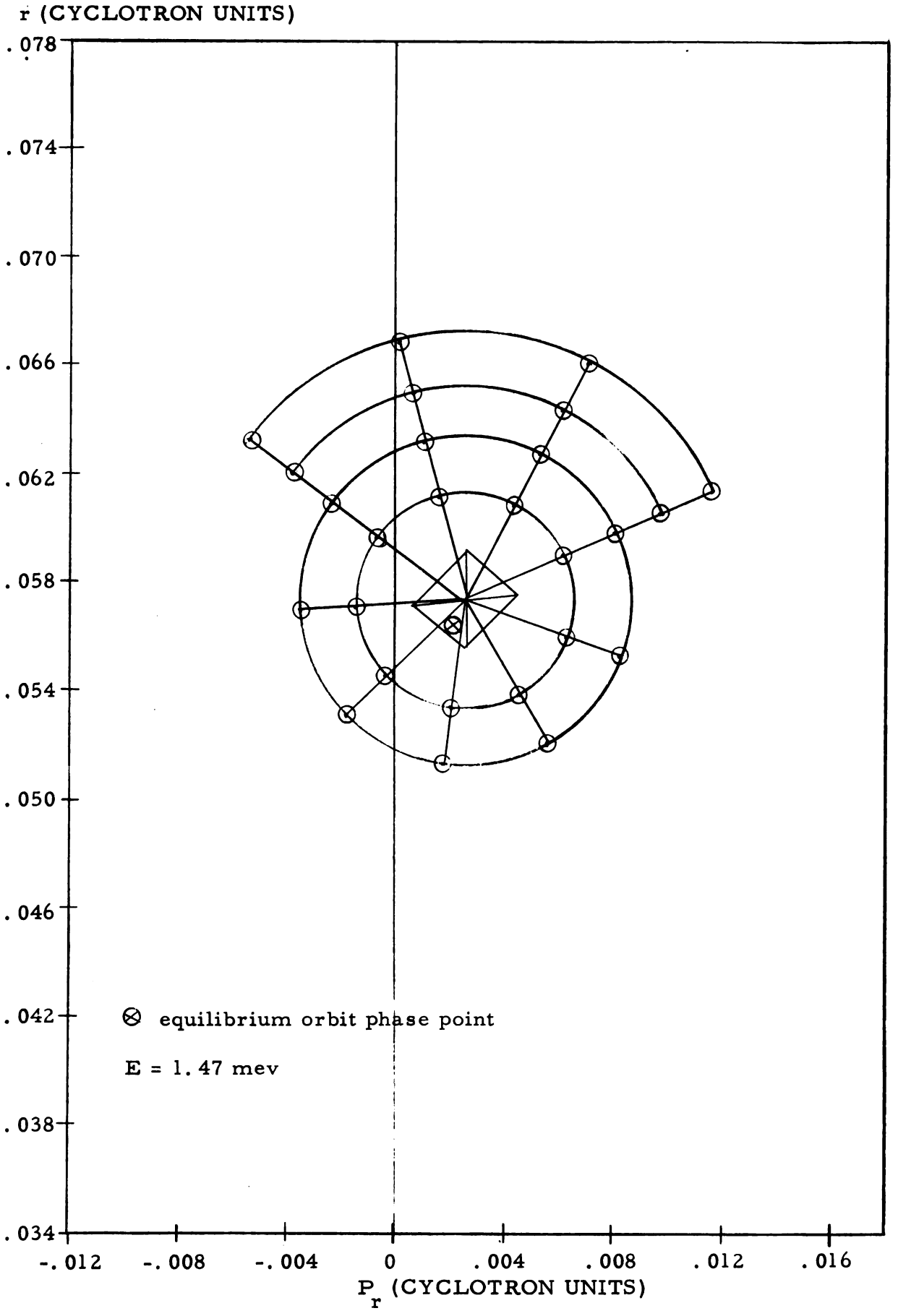

Figure 17. The initial conditions for protons accelerated and decelerated from resonance.

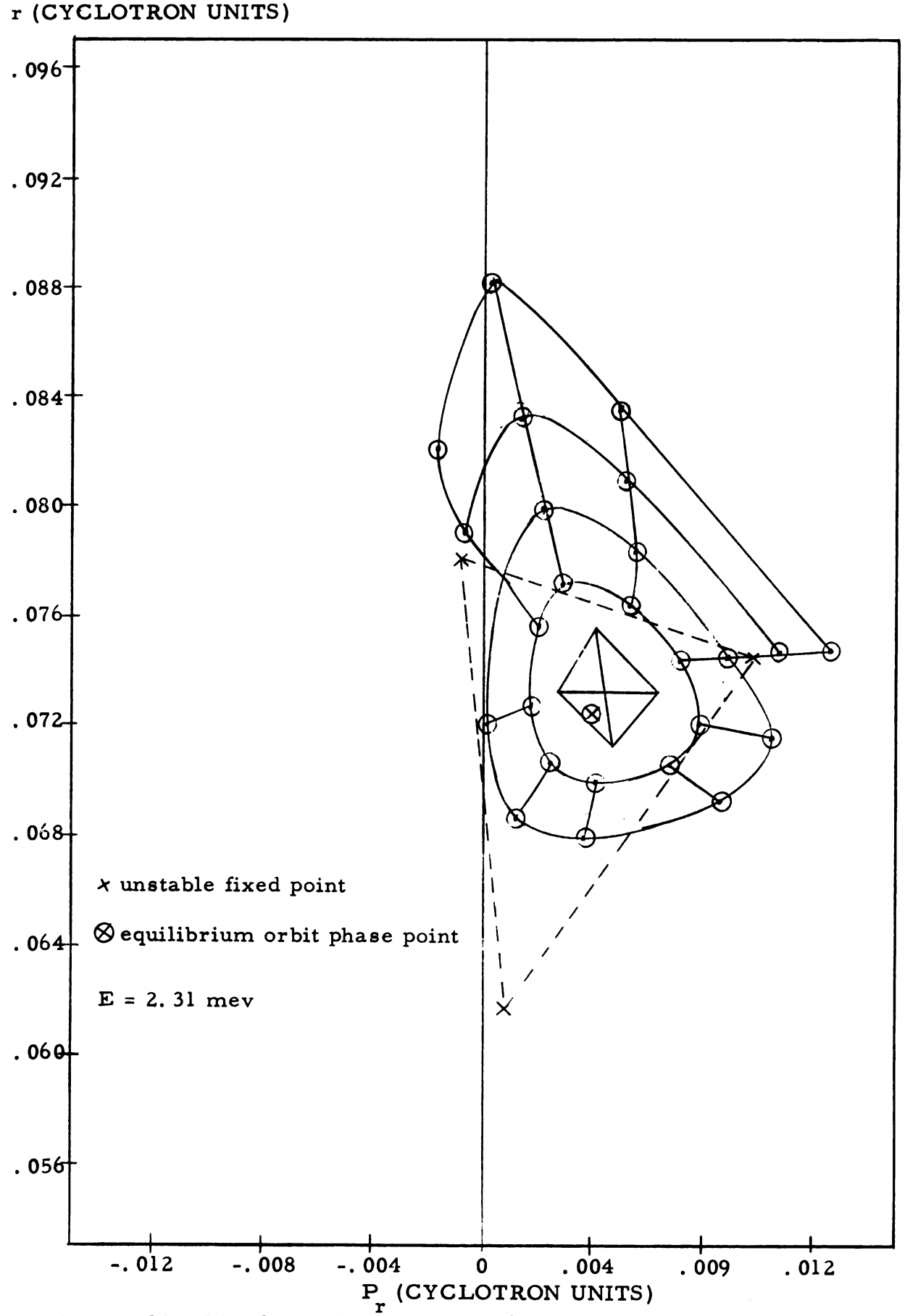

Figure 18. The distortion three revolutions above resonance.

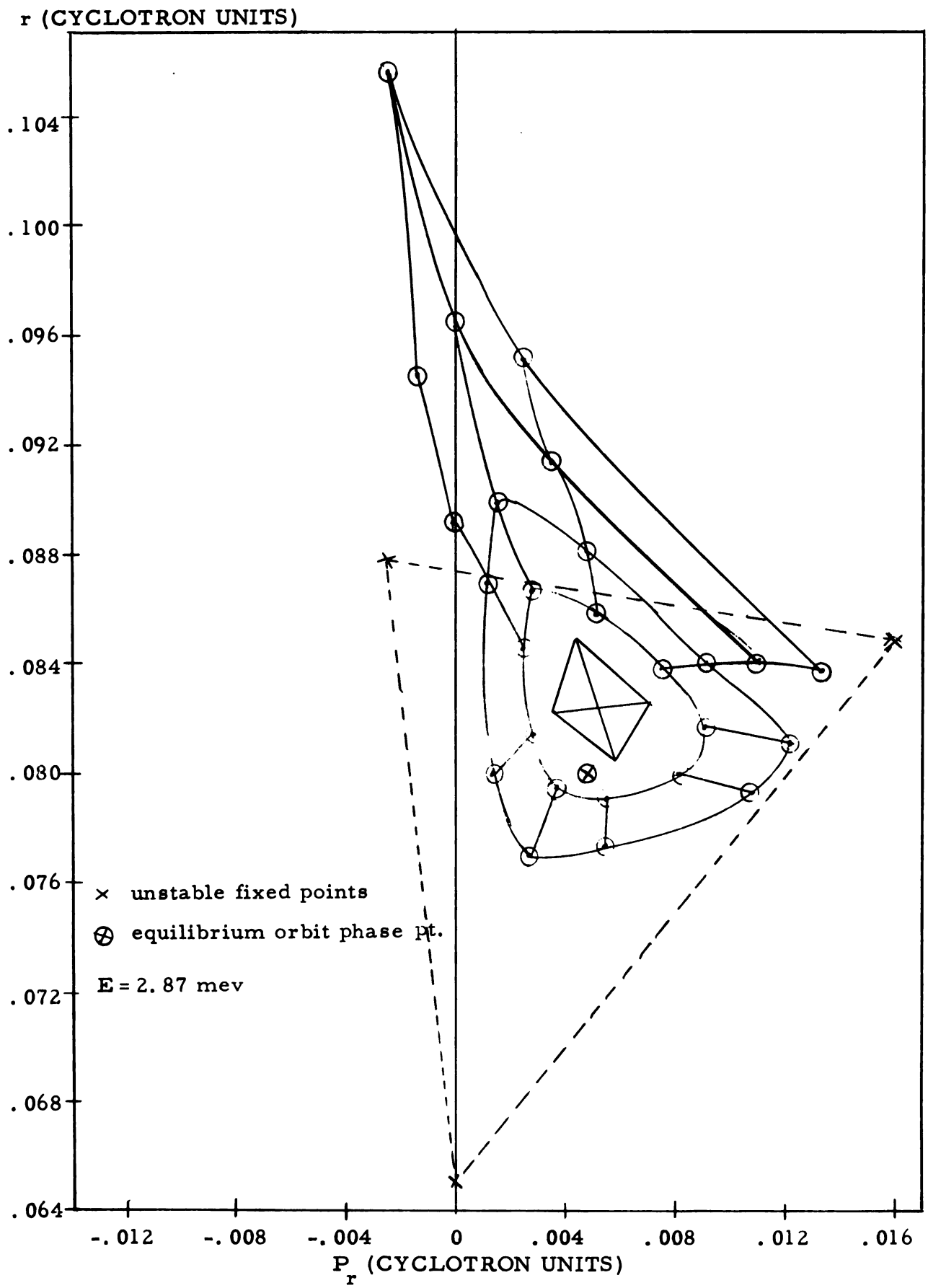

Figure 19. The distortion five revolutions above resonance.

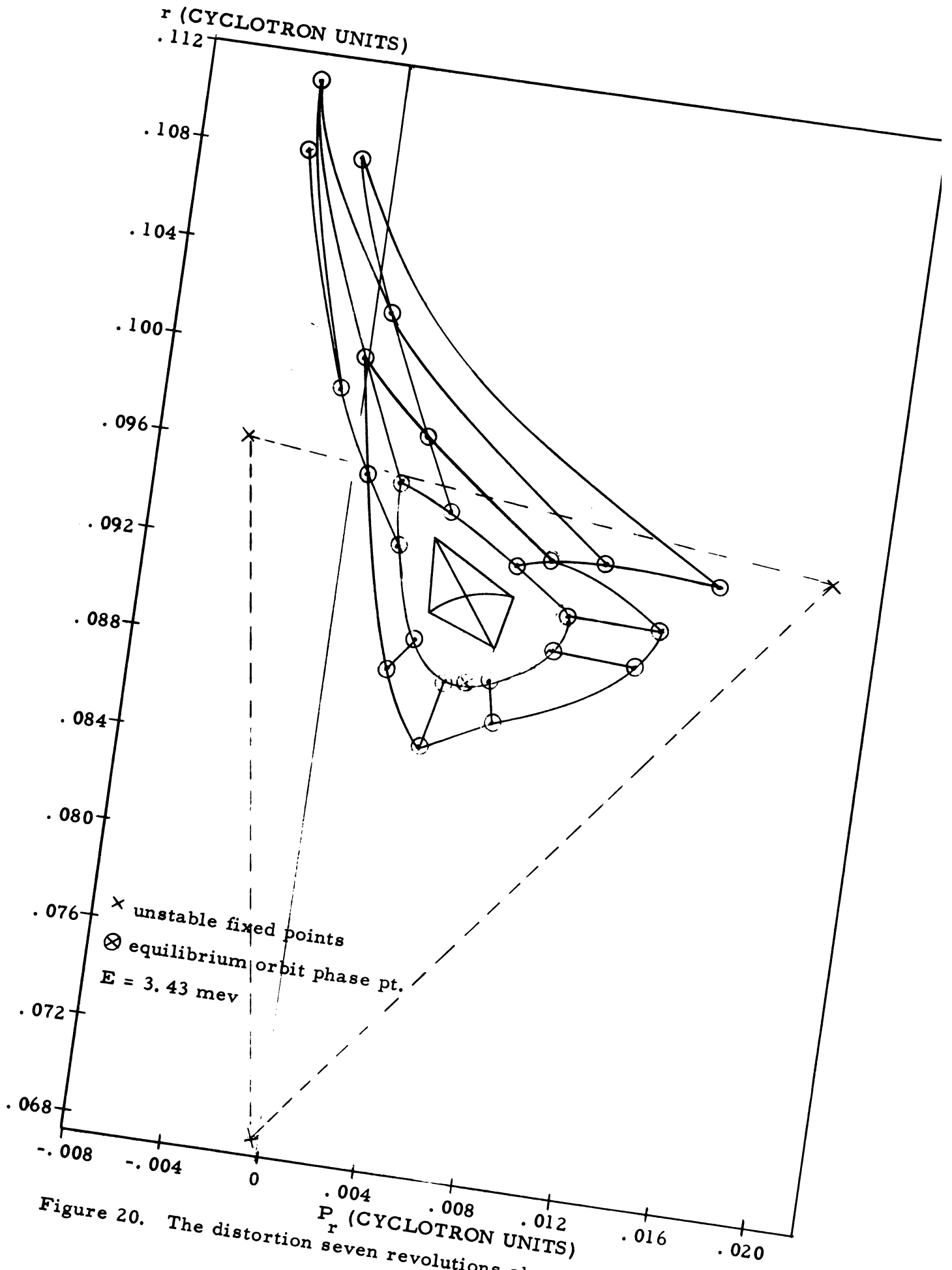

Figure 20. The distortion seven revolutions above reso

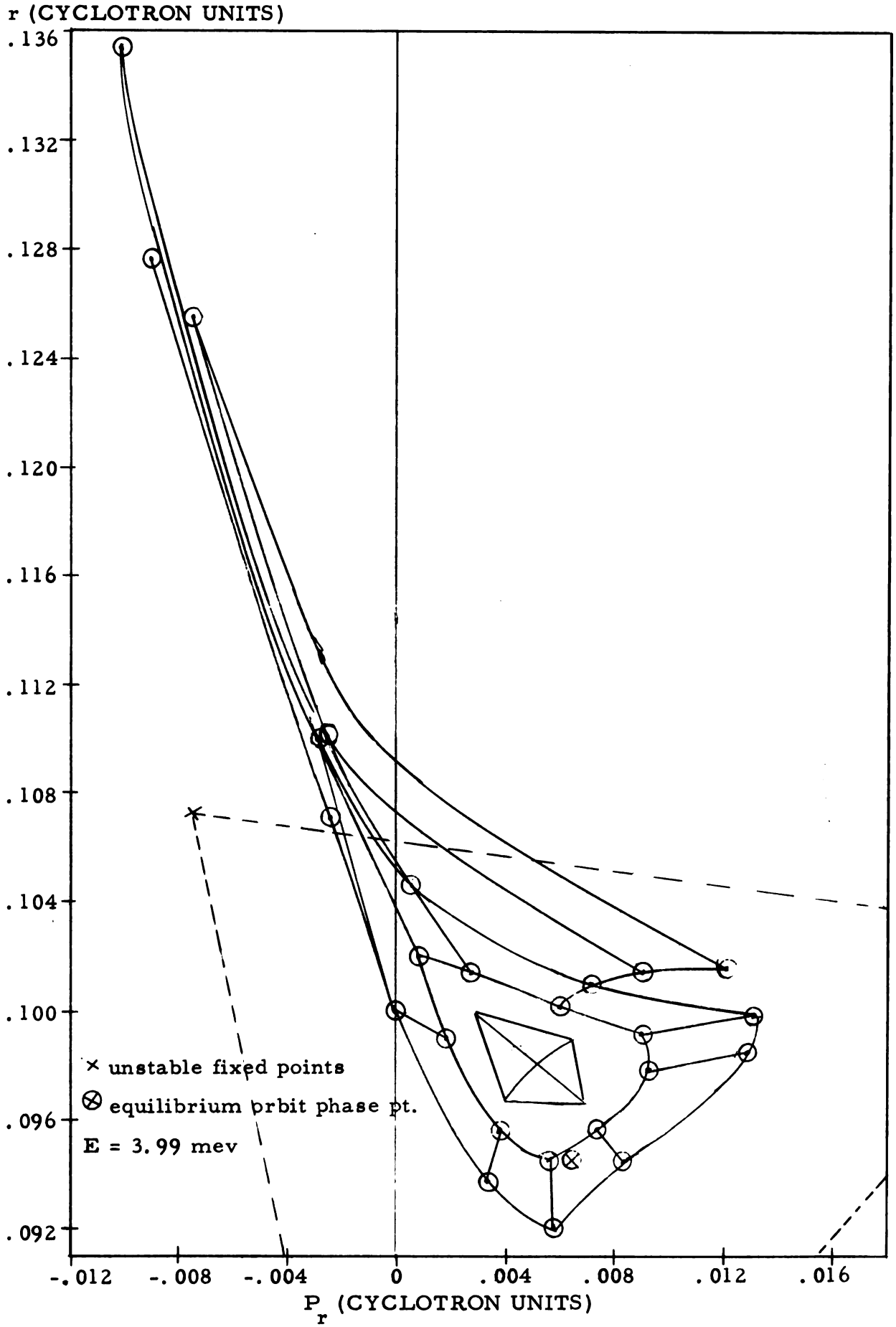

Figure 21. The distortion nine revolutions above resonance.

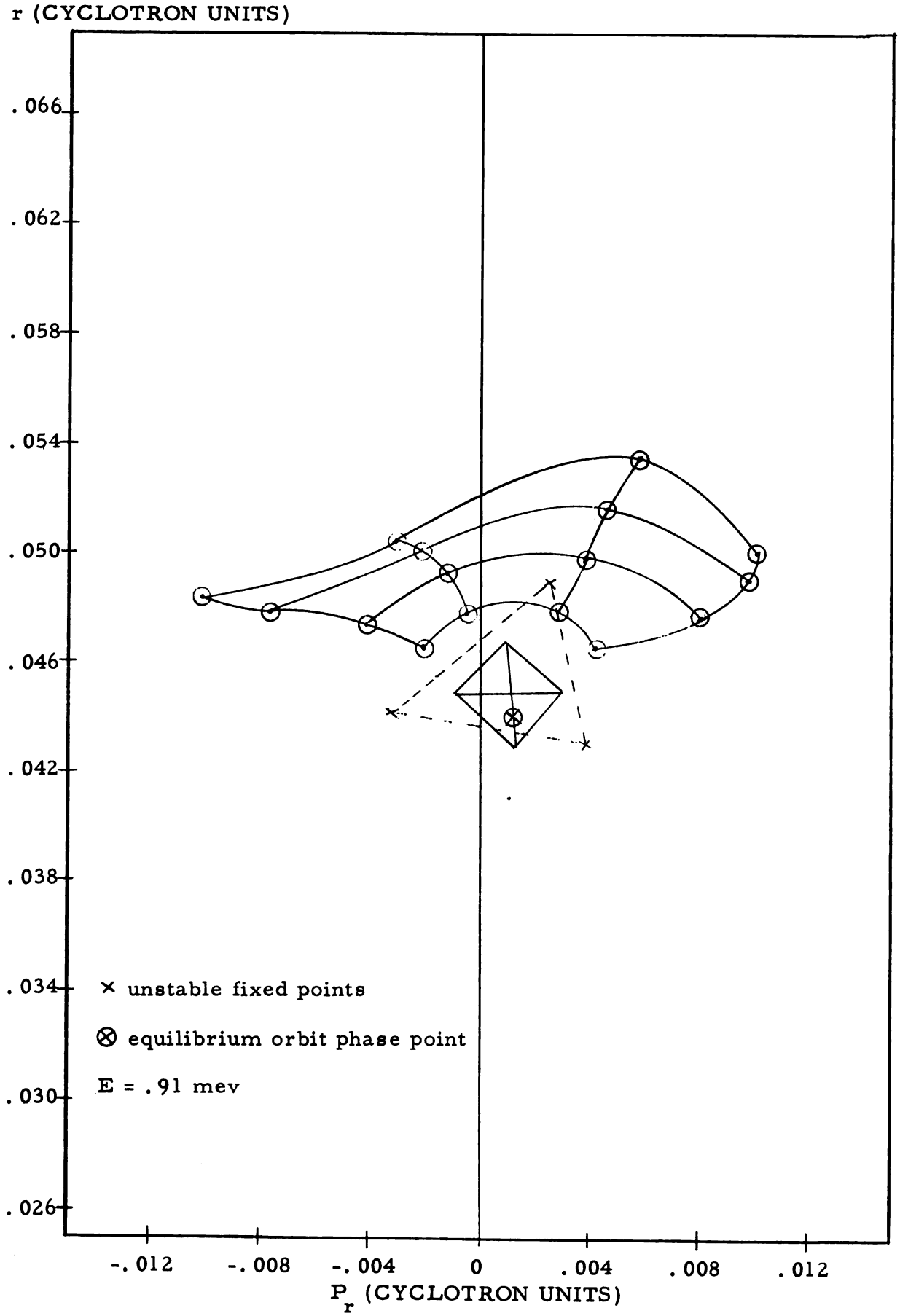

Figure 22. The distortion two revolutions below resonance.

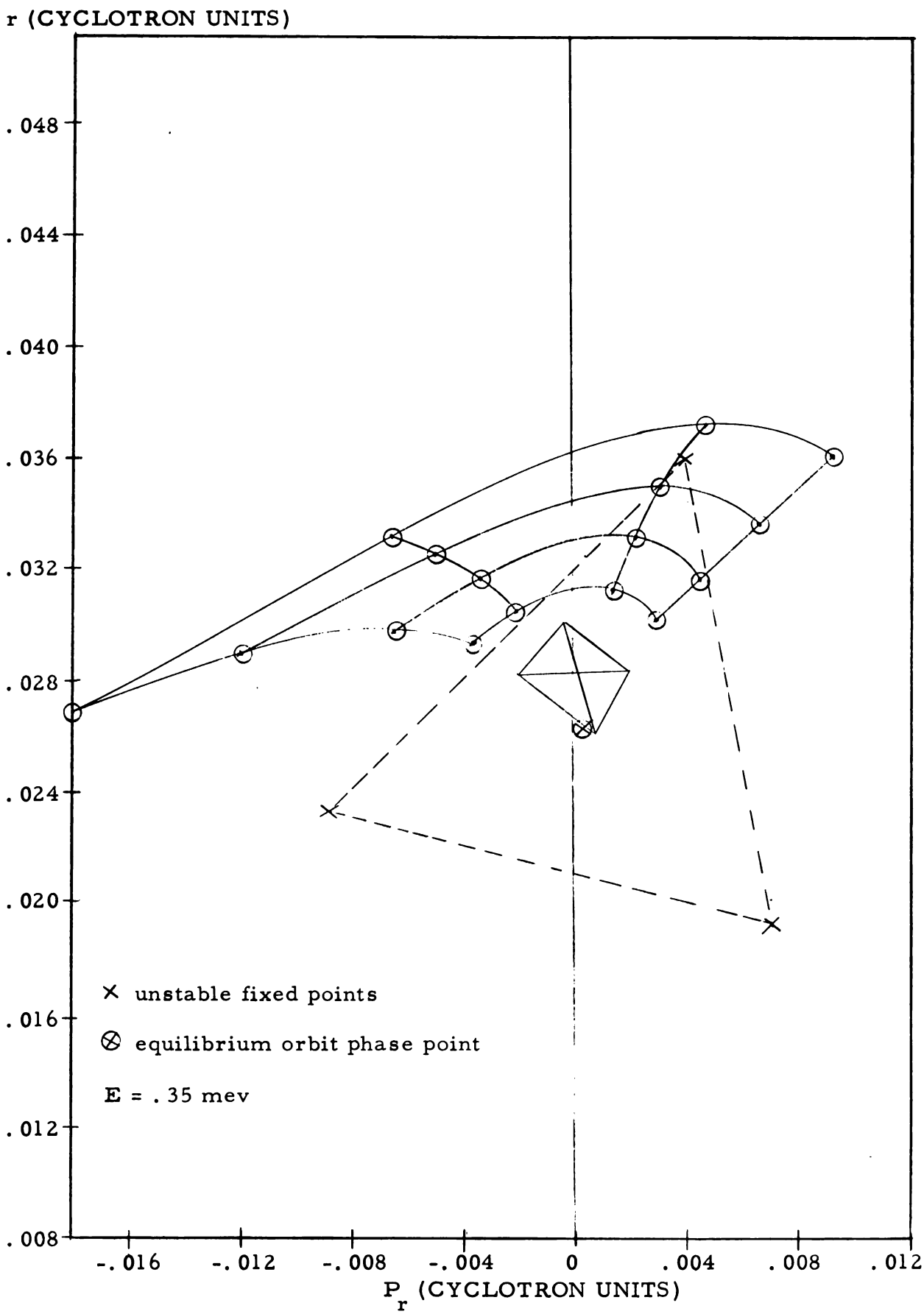

Figure 23. The distortion four revolutions below resonance.

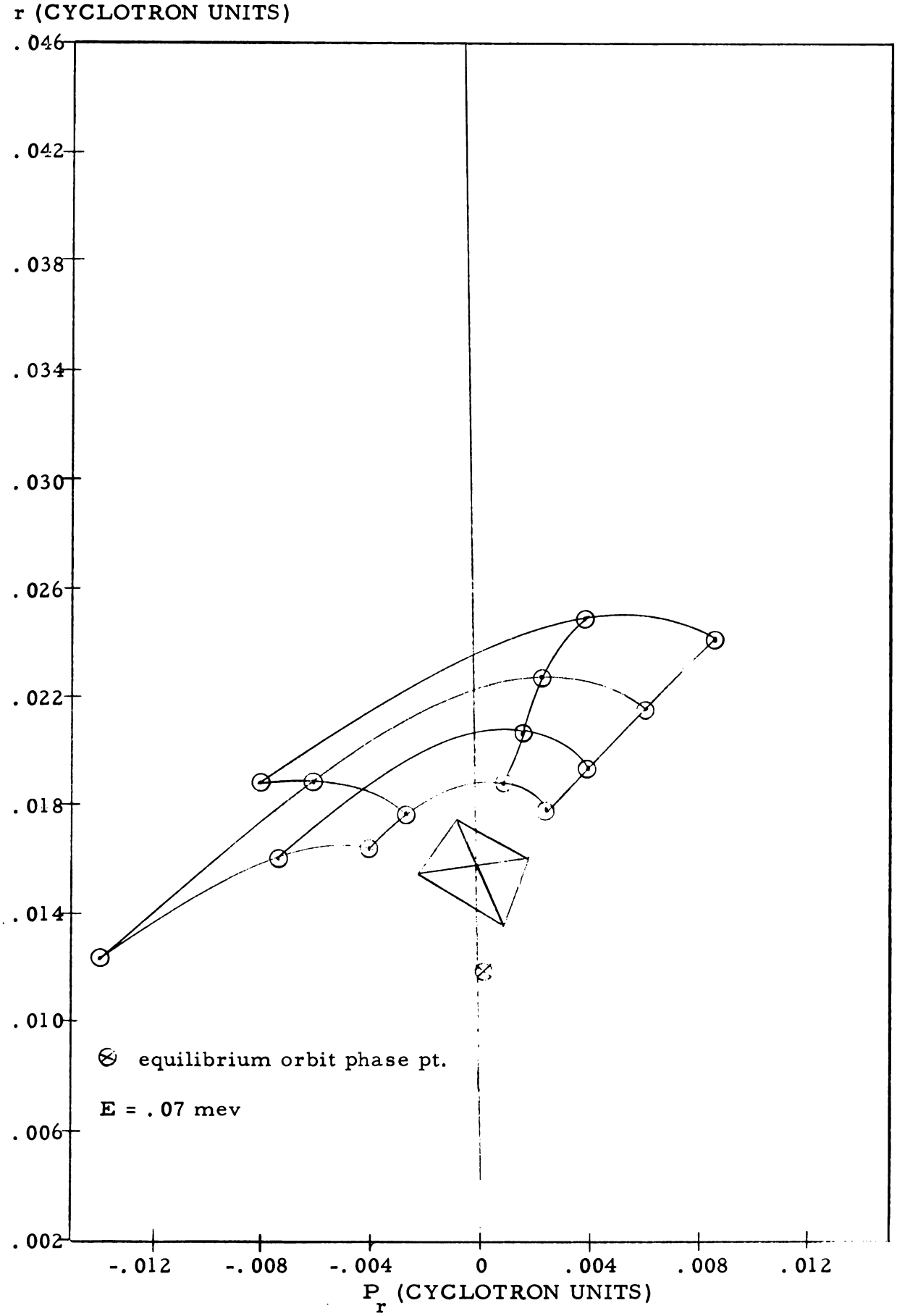

Figure 24. The distortion five revolutions below resonance.

CONCLUSION

Numerical calculations show that good axial focusing can be obtained near the center of a sector focused cyclotron from a non-isochronous average magnetic field without excessive phase slip. The average field given in Section I is especially designed for a proton with an energy gain per revolution of 280 kev in the azimuthally varying field shown in figure 1. The procedure described can be applied to other ions in simularly varying magnetic fields if the magnitude of the accelerating voltage is chosen properly.

Ions accelerated in the field described above must traverse the 3/3 radial resonance near the center of the cyclotron. The effects of this resonance must be carefully investigated for three sector cyclotrons. The feasibility of accelerating a practical-sized beam of protons through the 3/3 resonance without loss of particles or severe beam distortion is established in Sections II and III. It is shown by orbital integration with a digital computer that a 1/2 inch wide beam of protons with an energy gain per revolution of 280 kev can be accelerated through this resonance without intolerable beam distortion. This beam width is sufficiently large for the practical operation of a cyclotron.

APPENDIX

Radial Stability in the Central Region Due to Radial Variation in the Magnetic Field

A qualitative consideration of the trajectories of 70 kev protons initially displaced from their equilibrium orbit indicates that large amplitudes of radial oscillations are stable in the field considered here. The radius of the equilibrium orbit of 70 kev protons is less than 1/30 the radius of the magnetic field. As can be seen from figures 3 and 6, the effect of the azimuthal variation in the field can be neglected in comparison with the effect of the radial variation of the field. Since $\nu_r = .9855$ at this energy, the trajectories of ions with small initial displacements from the equilibrium orbit will form the rosette shaped patterns discussed in Section II. For larger radial amplitudes the trace of the trajectories, after a given revolution, deviate from circular as the ions sweep through the radial gradient of the magnetic hill centered at r = 0. However, the rosette shaped pattern is maintained for all trajectories which circumscribe the center of the field each revolution. If the initial radial displacement of an ion is such that its trajectory does not circumscribe the center of the field each revolution, then its trajectory forms a trochoid-like trace in the magnetic field gradient about the central hill. Since these trochoid shaped trajectories move along the equilibrium orbit the criterion for stability given by Courant and Snyder (10) is satisfied. That is,

an ion moving along such a trajectory will remain near the equilibrium orbit for all time.

As can be seen by a consideration of figures 1 and 6, only if a 70 kev proton's initial radial displacement from the equilibrium orbit is large in comparison to the radius of its equilibrium orbit will its trajectory form a trochoid-like trace which will move out radially in the manner described in Section II.

BIBLIOGRAPHY

(1) L. H. Thomas, Phys. Rev. 54, p. 580 (1938).

(2) D. W. Kerst and P. Serber, Phys. Rev. 60, 53 (1941).

(3) T. A. Heyn and Khoe Kong Tat, RSI 29, p. 622 (1958).

(4) S. Chatterjee, Private Communication.

(5) B. L. Cohen et al., Oak Ridge Relativistic Cyclotron, ORNL-2648.

(6) K. R. Symon et al., Phys. Rev. 103, p. 1837 (1956).

(7) T. Arnette, Michigan State University, unpublished (1960).

(8) H. G. Blosser, Michigan State University, unpublished (1960).

(9) M. M. Gordon and T. A. Welton, ORNL-2765.

(10) E. D. Courant and H. S. Snyder, Annals of Phys. 3, p. 1 (1958).

(11) H. G. Blosser, Sector Focused Cyclotrons, Submitted for publication in Proceedings of AIEE (1959).

(12) B. L. Cohen, Cyclotrons and Synchrocyclotrons, Handbuch der Physik, Vol. XLIV (1959).

(13) P. A. Sturroch, Annals of Phys. 3, p. 113 (1958).

(14) H. G. Blosser and M. M. Gordon, A Proposal to U.S. Atomic Energy Commission, Michigan State University publication (1959).

(15) H. Goldstein, Classical Mechanics, p. 266, Addison-Wesley Press, Cambridge (1951).

(16) P. H. Sturrock, Static and Dynamic Electron Optics, Cambridge Press (1955).

(17) H. G. Blosser et al., Proposal for a Nuclear Research Facility, Michigan State University publication (1958).